Advanced

Selected topics on perturbative approaches to large-scale structure

Perturbation theory (PT) of large-scale structure

Power spectrum / correlation function

Bispectrum / three-point correlation function

Power spectrum covariance

Modeling redshift-space distortions

Modeling galaxy bias

⋮

As long as we are interested in weakly nonlinear scales, PT calculation can be applied to a practical use of theoretical template

However,…

UV problem in PT

Basic eqs. for perturbation theory

Starting point

single-stream approximation of collisionless Boltzmann eq.

Phase-space distribution function

$$f(\boldsymbol{x},\, \boldsymbol{v};\, t) \rightarrow \overline{\rho}(t)\, \{1+\delta(\boldsymbol{x};\, t)\}\, \delta_{\rm D}\left(\boldsymbol{v}-\boldsymbol{v}(\boldsymbol{x};\, t)\right)$$

<u>Basic eqs.</u>

$$\frac{\partial \delta}{\partial t}+\frac{1}{\mathrm{a}}\vec{\nabla}\cdot\left[(1+\delta)\vec{\mathrm{v}}\right]=0$$

$$\frac{\partial\, \vec{\mathrm{v}}}{\partial t}+\frac{\dot{a}}{a}\vec{\mathrm{v}}+\frac{1}{a}(\vec{\mathrm{v}}\cdot\vec{\nabla})\,\vec{\mathrm{v}}=-\frac{1}{a}\vec{\nabla}\,\Phi$$

$$\frac{1}{a^2}\nabla^2\Phi=4\pi G\,\overline{\rho}_{\mathrm{m}}\,\delta$$

<u>PT expansion</u>

Assuming the irrotational flow

$$\delta=\delta^{(1)}+\delta^{(2)}+\cdots$$

$$\theta=\theta^{(1)}+\theta^{(2)}+\cdots$$

$$\theta\equiv\frac{\nabla\cdot\vec{v}}{a\,H}$$

PT kernels

initial density field

$$\delta^{(n)}(\boldsymbol{k};t) = \int \frac{d^3\boldsymbol{k}_1 \cdots d^3\boldsymbol{k}_n}{(2\pi)^{3(n-1)}}\,\delta_{\rm D}(\boldsymbol{k}-\boldsymbol{k}_{12\cdots n})\boxed{F_n(\boldsymbol{k}_1,\cdots,\boldsymbol{k}_n;\,t)}\,\delta_0(\boldsymbol{k}_1)\cdots\delta_0(\boldsymbol{k}_n),$$

$$\theta^{(n)}(\boldsymbol{k};t) = \int \frac{d^3\boldsymbol{k}_1 \cdots d^3\boldsymbol{k}_n}{(2\pi)^{3(n-1)}}\,\delta_{\rm D}(\boldsymbol{k}-\boldsymbol{k}_{12\cdots n})\boxed{G_n(\boldsymbol{k}_1,\cdots,\boldsymbol{k}_n;\,t)}\,\delta_0(\boldsymbol{k}_1)\cdots\delta_0(\boldsymbol{k}_n),$$

EdS approximation:

D_+ : linear growth factor

$f=\dfrac{d\ln D_+}{d\ln a}$: growth rate

$$F_n \longrightarrow [D_+(t)]^n\,\boxed{\tilde{F}_n(\boldsymbol{k}_1,\cdots,\boldsymbol{k}_n)}$$

$$G_n \longrightarrow -f(t)\,[D_+(t)]^n\,\boxed{\tilde{G}_n(\boldsymbol{k}_1,\cdots,\boldsymbol{k}_n)}$$

Kernels $(\tilde{F}_n,\ \tilde{G}_n)$ are derived from recursion relations

Goroff et al. ('86)

➡ used to compute power spectrum, bispectrum, ...

Power spectrum

$$P(k) = \underbrace{P_{\rm lin}(k;t)}_{\text{Linear}} + \underbrace{P_{13}(k;t) + P_{22}(k;t)}_{\text{1-loop}} + \cdots$$

$$\int_{\boldsymbol{q}} \equiv \int \frac{d^3\boldsymbol{q}}{(2\pi)^3}$$

$$P_{\rm lin}(k;t) = [D_+(t)]^2\, P_0(k)$$

$$P_{22}(k) \;=\; 2\int_{\boldsymbol{q}} P_{lin}(q) P_{lin}(|\boldsymbol{k}-\boldsymbol{q}|)\, F_2^2(\boldsymbol{q}, \boldsymbol{k}-\boldsymbol{q}),$$

$$P_{13}(k) \;=\; 6P_{lin}(k)\int_{\boldsymbol{q}} P_{lin}(q)\, F_3(\boldsymbol{k}, \boldsymbol{q}, -\boldsymbol{q}),$$

Diagrams

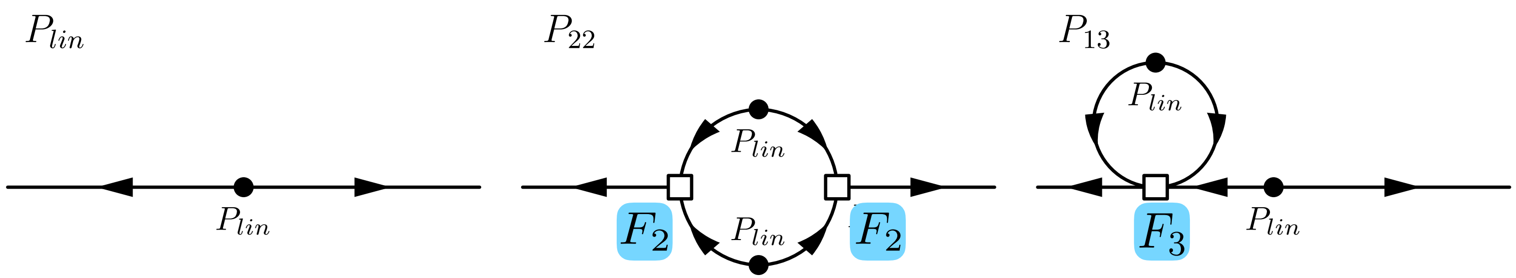

Asymptotic properties

For fixed total sum k, Goroff et al. ('86)

$$\lim_{q\to\infty} F_n(\boldsymbol{k}_1,\ldots,\boldsymbol{k}_{n-2},\boldsymbol{q},-\boldsymbol{q}) \propto \frac{k^2}{q^2}$$

$$\lim_{q\to\infty} F_2(\boldsymbol{q},\boldsymbol{k}-\boldsymbol{q}) \propto \frac{k^2}{q^2} \qquad \lim_{q\to\infty} F_3(\boldsymbol{k},\boldsymbol{q},-\boldsymbol{q}) \propto \frac{k^2}{q^2}$$

Low-k behavior of 1-loop corrections:

high-q limit

$$P_{22}(k)\Big|_{q\to\infty} \propto k^4 \int dq\, q^2\, \frac{P_{lin}^2(q)}{q^4}$$

$$P_{13}(k)\Big|_{q\to\infty} \propto P_{lin}(k)\, k^2 \int dq\, q^2\, \frac{P_{lin}(q)}{q^2}$$

P_{13} becomes dominant at k<<1 and scales as k^2

UV sensitive terms

For higher-loops,

$P_{15},\ P_{17},\ P_{19},\ \cdots$ become dominant at low-k and scale as k^2

$$\Rightarrow\quad P_{n\text{-loop}}(k)\ \sim\ P_{1(2n+1)}(k)$$

$$P_{1(2n+1)}(k) = 2\cdot(2n+1)!!\ P_{\rm lin}(k)$$
$$\times \int d^3\boldsymbol{q}_1\cdots d^3\boldsymbol{q}_n\ F_{2n+1}(\boldsymbol{k},\boldsymbol{q}_1,-\boldsymbol{q}_1,\cdots,\boldsymbol{q}_n,-\boldsymbol{q}_n)\, P_{\rm lin}(q_1)\cdots\times\ P_{\rm lin}(q_n)$$

logarithmically divergent (q>>1)

$$\overset{k\ll q_i}{\propto}\quad k^2\,P_{\rm lin}(k)\underline{\underline{\int\frac{dq}{2\pi^2}\,P_{\rm lin}(q)\,[\sigma_L(q)]^{2(n-1)}\,;}}\quad [\sigma_L(q)]^2\equiv\int_0^q\boxed{\frac{dq'\,q'^2}{2\pi^2}\,P_{\rm lin}(q')}$$

getting sensitive to large-q contribution
for higher loop (n↗)

Blas et al. ('14)

Loop corrections at z=0

Blas et al. JCAP 01 ('14) 010

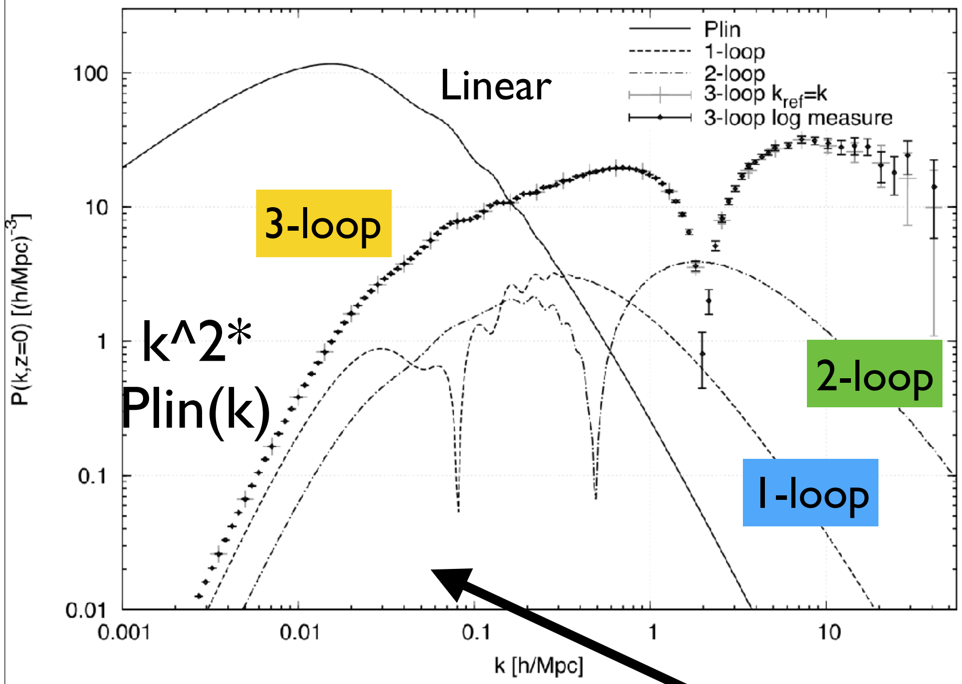

Figure 1: One, two and three-loop contributions to the equal-time power spectrum obtained from a numerical Monte Carlo integration within standard perturbation theory at $z = 0$. The linear power spectrum is obtained from the initial power spectrum from CAMB [20] using the ΛCDM model with WMAP5 parameters. For the three-loop order, the error bars show an estimate for the numerical error obtained by multiplying the error output of the CUBA routine Suave by a factor of two. The relative error is ≤ 0.002 for $k \leq 0.55$ h/Mpc. The black diamonds and grey crosses correspond to two different parametrizations of the absolute loop momenta (see App. A).

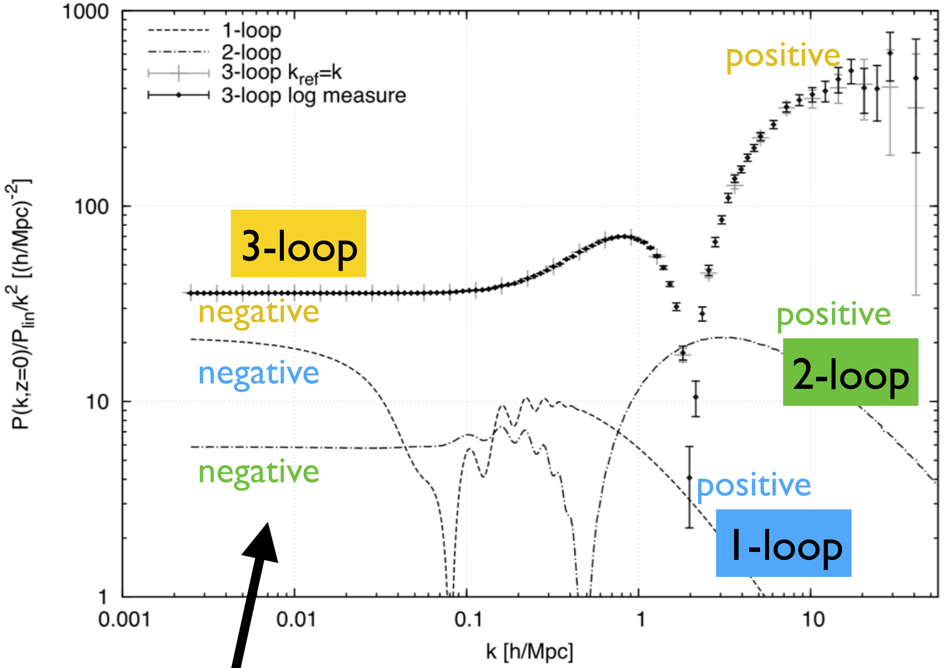

Figure 4: Ratio $P_{L-loop}(k, z = 0)/P_{lin}(k, z = 0)/k^2$ for the one- two- and three-loop contributions (line styles as in Fig. 1).

P13, P15, P17 give a major contribution

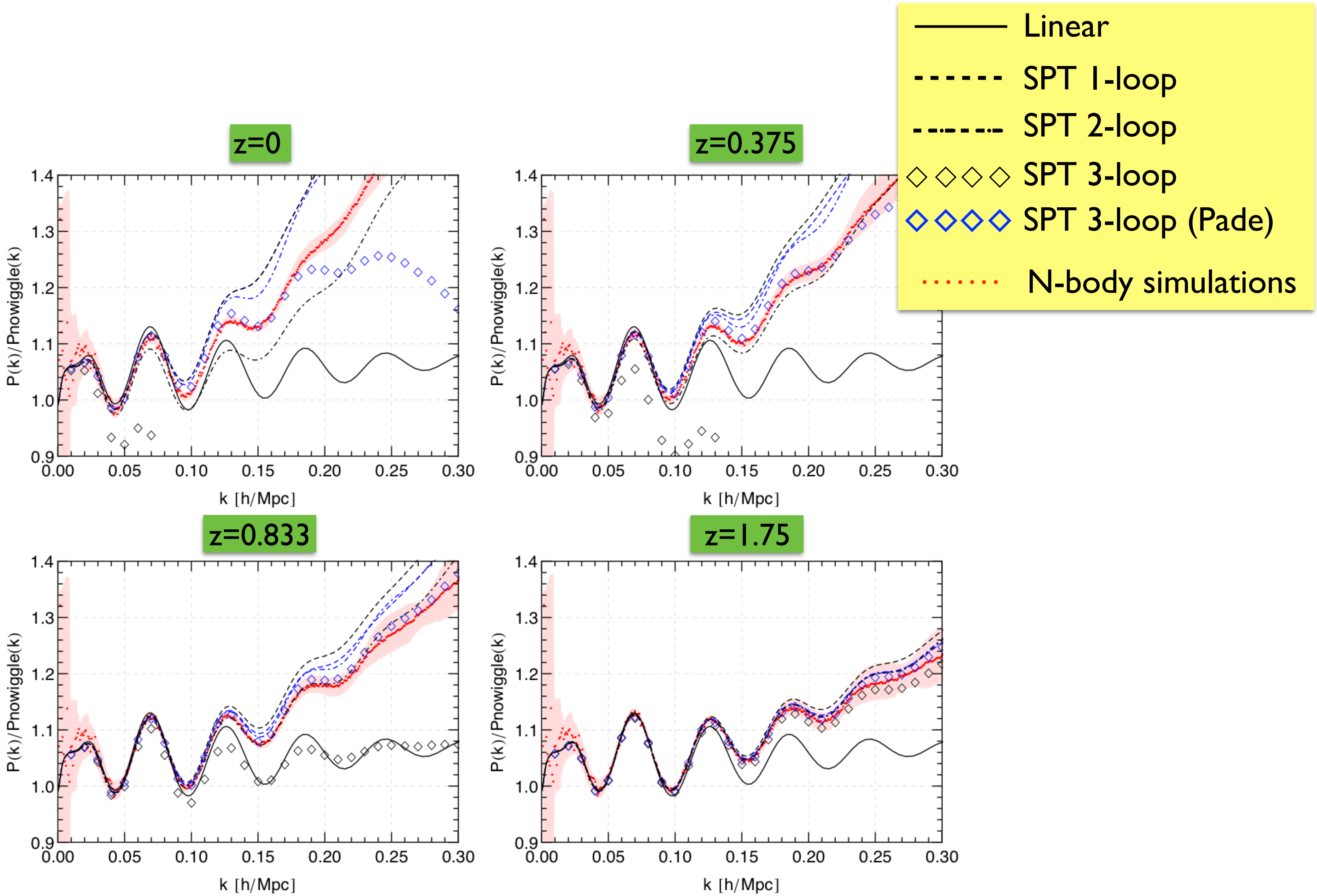

Blas et al. JCAP 01 ('14) 010

Ubiquitous UV sensitivity

For bispectrum,

1-loop

$$B(k_1,k_2,k_3) = B_{112} + \underline{[B_{114} + B^{I}_{123} + B^{II}_{123} + B_{222}]} + \cdots$$

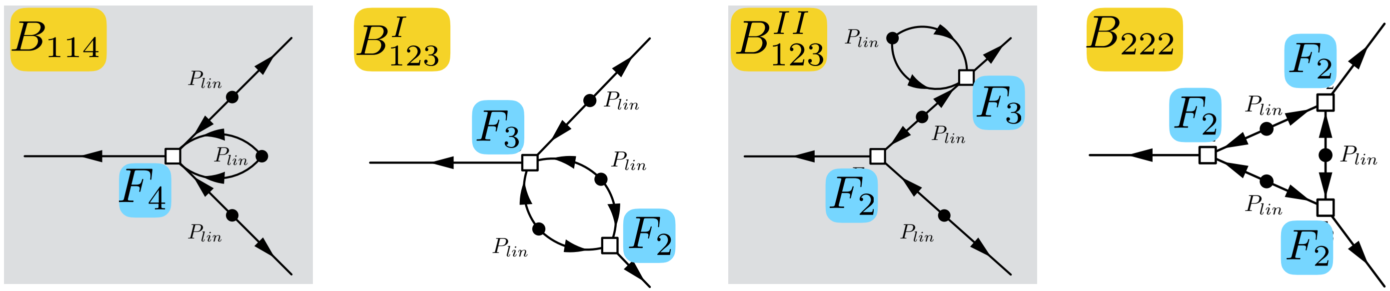

For $k_1 \sim k_2 \sim k_3$, low-k behavior is dominated by B_{114} and B^{II}_{123}

and scales as k^2 (Baldauf et al. '15a)

In general, $B^{n\text{-loop}} \overset{k_i \ll 1}{\sim} B_{11(2n+2)},\quad B^{II}_{12(2n+1)}$

$$\propto\ k^2\,[P_{\rm lin}(k)]^2 \int \underline{\frac{dq}{2\pi^2}\,P_{\rm lin}(q)\,[\sigma_L(q)]^{2(n-1)}}$$

UV sensitive for higher loop (n↗)

Mitigating UV sensitivity

UV sensitivity is not a real physical effect

$\longrightarrow$ needs to be cured for an improved prediction

EFT approach

add counter terms to mitigate UV sensitivity

For P(k) at 1-loop order,

free parameter

counter term to be added : $-c_s^2 k^2 P_{\rm lin}(k)$

This corresponds to adding $\underline{\underline{-c_s^2 \nabla \delta}}$ at RHS of Euler eq.

effective pressure $\longrightarrow$ c_s : *'sound velocity'*

$$\frac{\partial \vec{v}}{\partial t} + \frac{\dot{a}}{a}\vec{v} + \frac{1}{a}(\vec{v}\cdot\vec{\nabla})\vec{v} = -\frac{1}{a}\vec{\nabla}\Phi \quad -\frac{1}{\rho_{\rm m}}\nabla\tau_{ij}$$

$$\tau_{ij} = \rho_{\rm m}\left[\left(c_{\rm s}^2\,\delta - \frac{c_{\rm bv}^2}{aH}\,\nabla\cdot\boldsymbol{v}\right)\delta_{ij} - \frac{3}{4}\frac{c_{\rm sv}^2}{aH}\left\{\partial_j v_i + \partial_i v_j - \frac{2}{3}(\nabla\cdot\boldsymbol{v})\delta_{ij}\right\}\right] + \cdots$$

Power spectrum in EFT

Baldauf et al. ('15b)

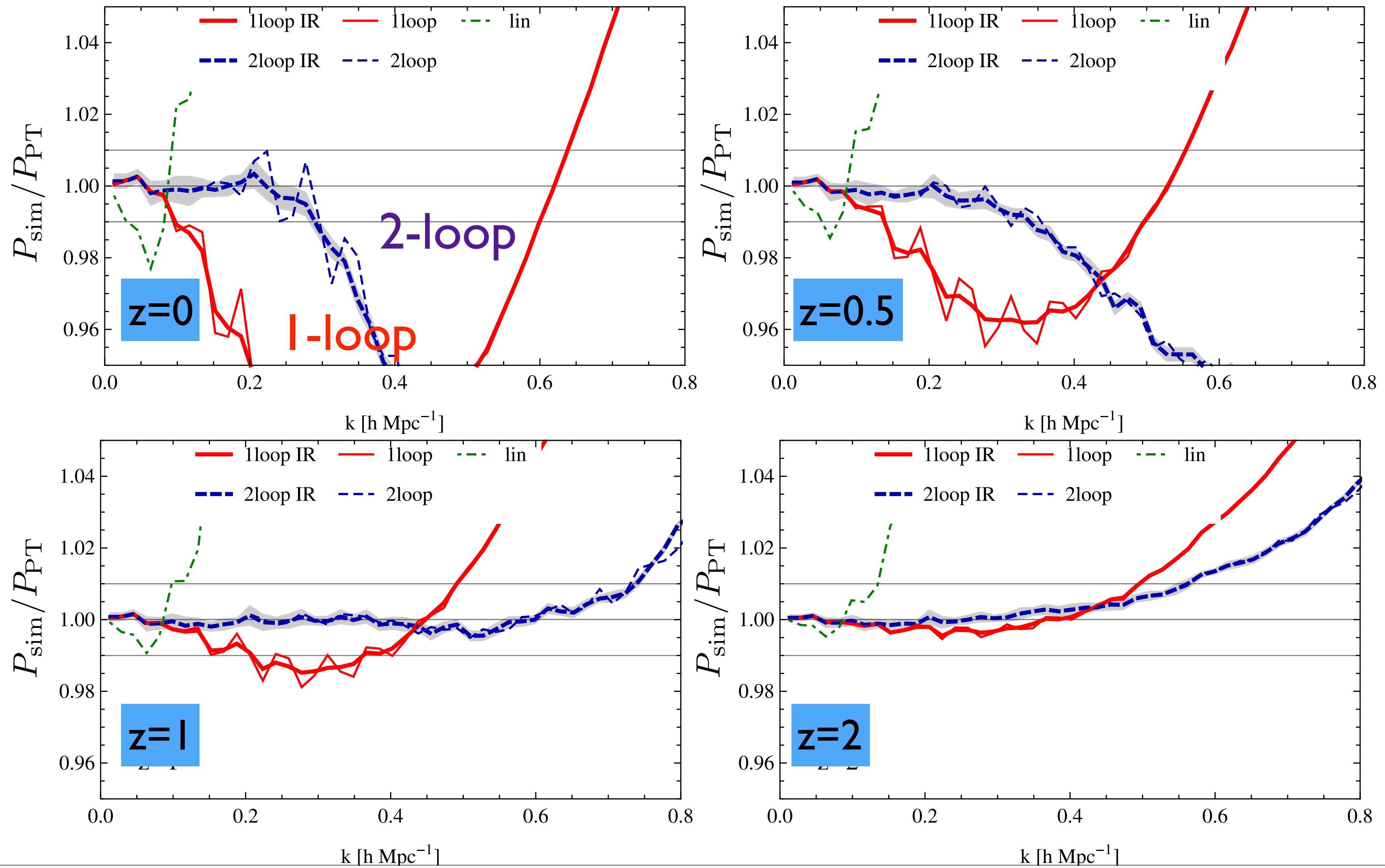

(c.f.) resummed PT w/o EFT

RegPT including *next-to-next-to-leading order*

$L_{\mathrm{box}} = 2,048\,h^{-1}\,\mathrm{Mpc}$
# of particles : $1,024^3$
# of runs : 60
cosmology : wmap5

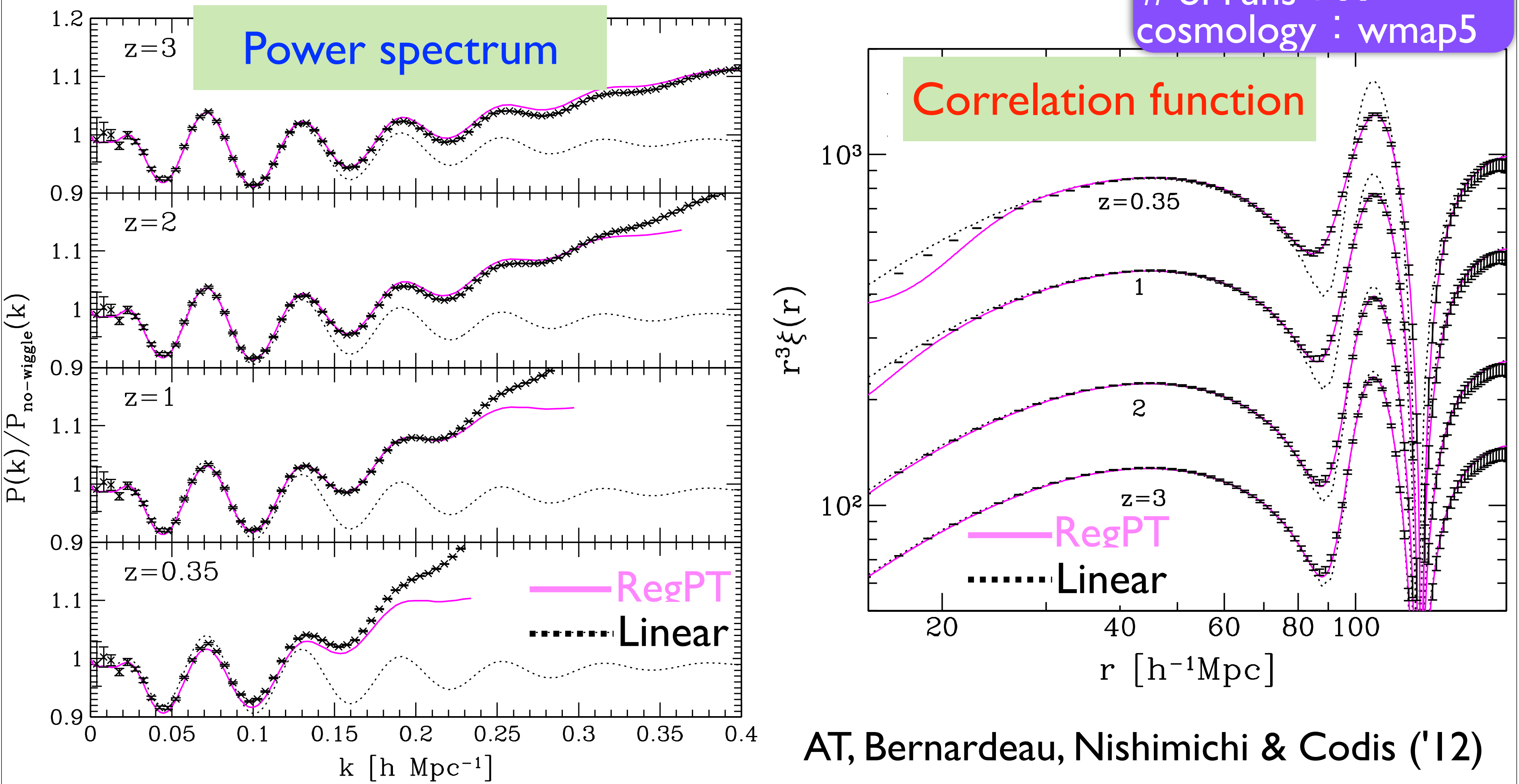

AT, Bernardeau, Nishimichi & Codis ('12)

Critical comments

- The size of each counter term is unknown, and it needs to be calibrated with N-body simulations

  e.g., $c_s \sim 1\,h^{-1}\,\mathrm{Mpc}$ (but, it generally depends on time & cosmology)

- At 2-loop order, counter terms for sub-leading corrections also need to be considered, increasing # of free parameters

- For bispectrum at 1-loop order, we generally need <u>3 types of counter terms</u>, in addition to the one introduced in P(k)

(Baldauf et al. '15a)

Physical origin or meaning of each counter term is unclear

Response function of large-scale structure to small-scale fluctuations

Nishimichi, Bernardeau & AT, Phys.Lett.B 762 (2016) 247
arXiv:1411.2970

3-loop : source of trouble

Further including 3-loop (i.e., next-to-next-to-next-to-leading order),
PT calculations start to get worse !!

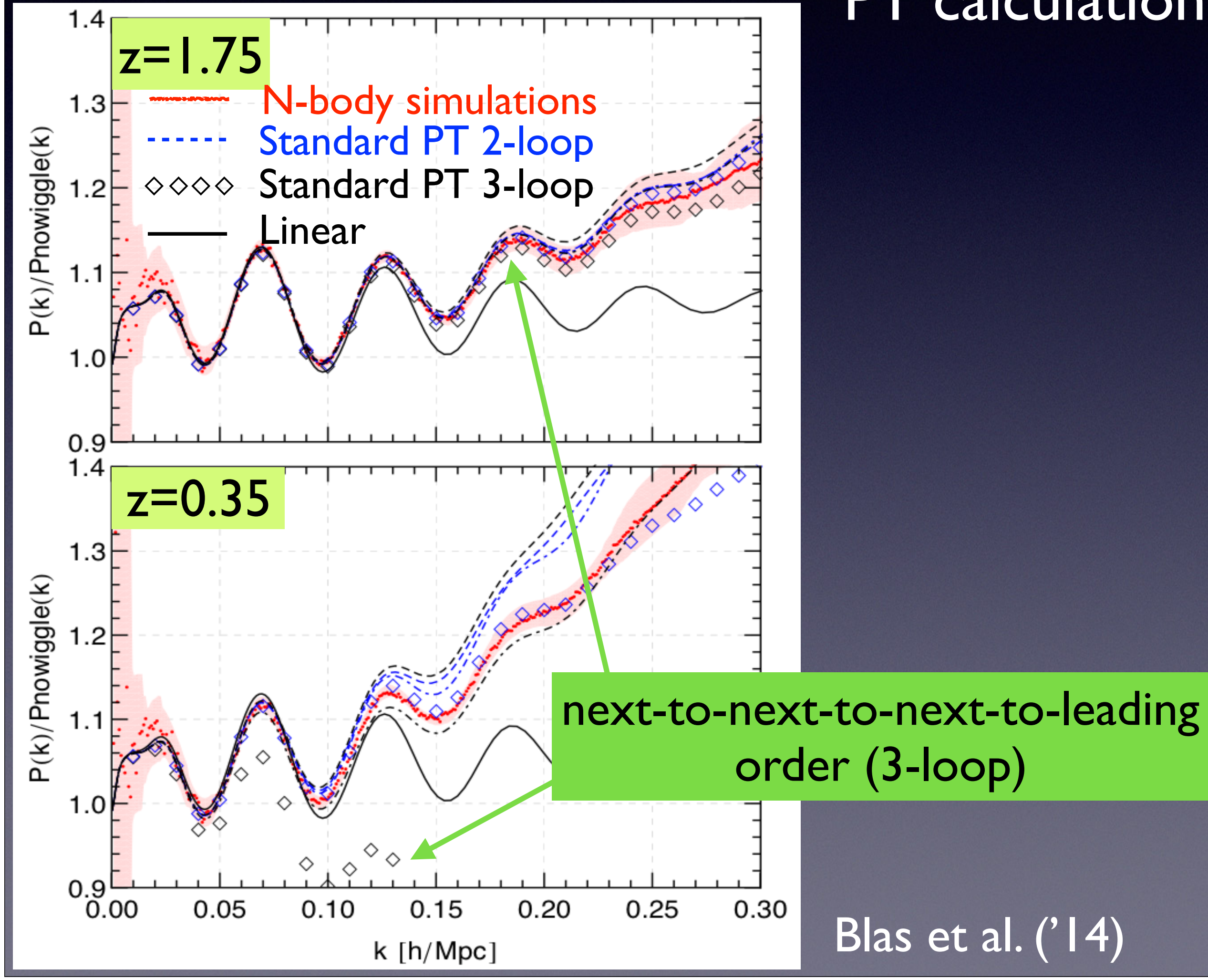

Blas et al. ('14)

3-loop : source of trouble

Further including 3-loop (i.e., next-to-next-to-next-to-leading order),
PT calculations start to get worse !!

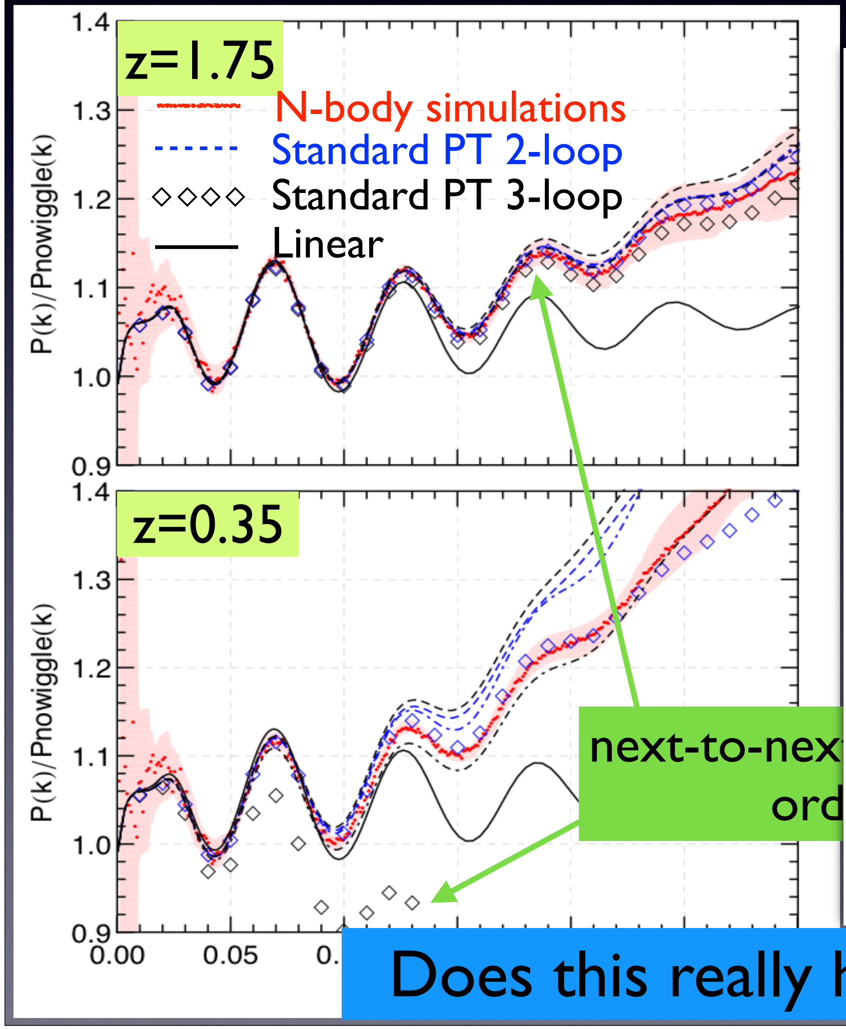

$$P_{\text{n-loop}}(k) \propto \int d\ln q \; K_{\text{n-loop}}(k,q)\, P_0(q)$$

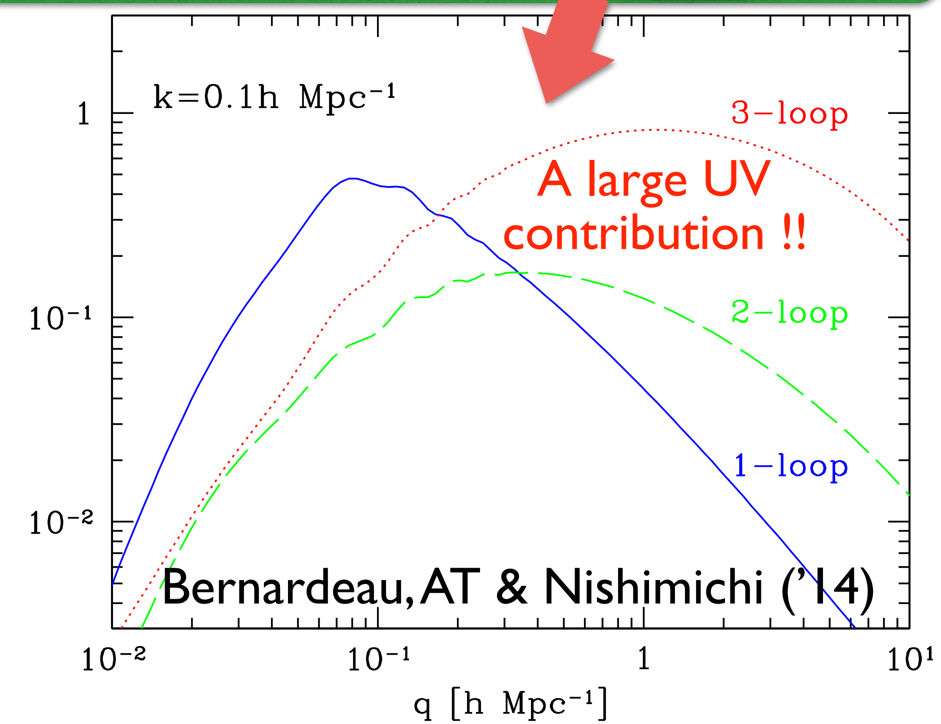

Does this really happen in real universe ?

Nature of nonlinear mode-coupling

How the small-scale fluctuations affect the evolution of large-scale modes ? (or vice versa)

How the small disturbance added in <u>initial power spectrum</u> can contribute to each Fourier mode in <u>final power spectrum ?</u>

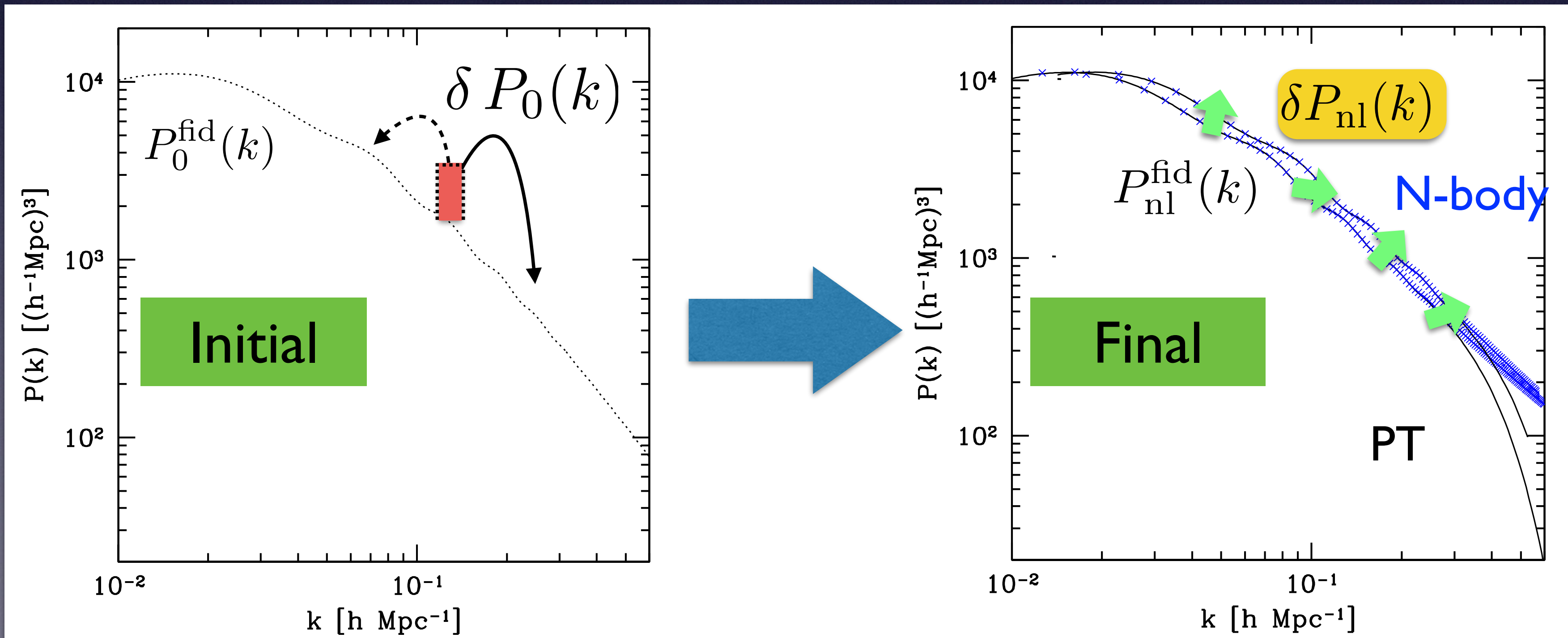

Nature of nonlinear mode-coupling

How the small-scale fluctuations affect the evolution of large-scale modes ? (or vice versa)

How the small disturbance added in <u>initial power spectrum</u> can contribute to each Fourier mode in <u>final</u> ... <u>ctrum ?</u>

Response function

$$\delta P_{\rm nl}(k) = \int d\ln q\, K(k,q)\, \delta P_0(q)$$

Final (nonlinear)

initial (linear)

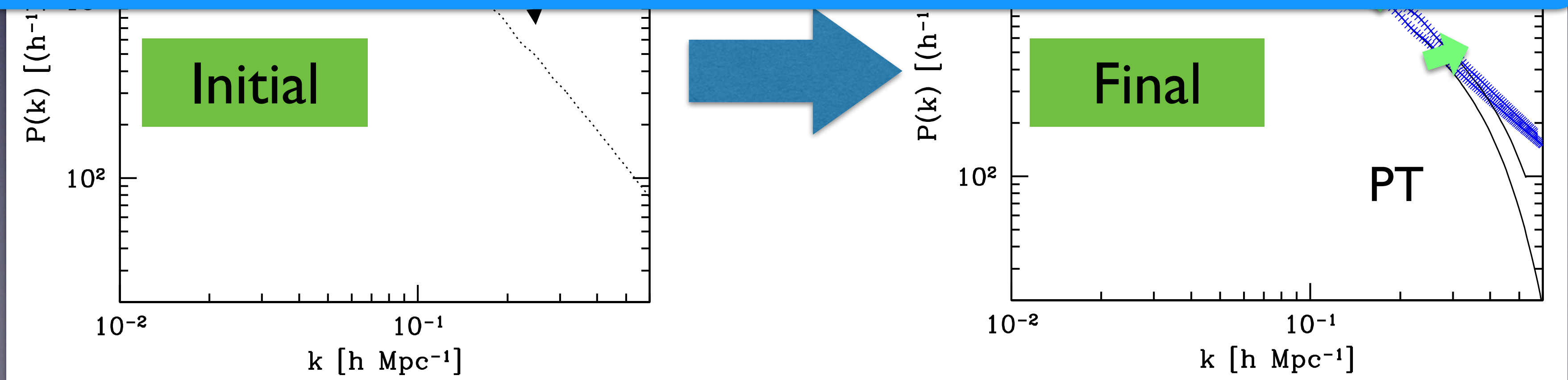

Measurement of kernel

Definition in terms of functional derivative :

$$K(k,q) = q\,\frac{\delta P_{\rm nl}(k)}{\delta P_0(q)}$$

Estimator for mode-coupling kernel (discretized):

$$\widehat{K}(k_i,q_j)\,P_0(q_j) \equiv \frac{P^+_{\rm nl}(k_i) - P^-_{\rm nl}(k_i)}{\Delta\ln P_0\,\Delta\ln q} \quad ; \quad \begin{array}{l}\Delta\ln q \\ = \ln q_{j+1} - \ln q_j\end{array}$$

$P^{\pm}_{\rm nl}(k)$: Final output of non-linear power spectrum, for which a small perturbation $P^{\pm}_{0,j}(k)$ is added in initial power spectrum, $P_0(k)$

$$\ln\left[\frac{P^{\pm}_{0,j}(q)}{\ln P_0(q)}\right] = \begin{cases} \pm\frac{1}{2}\Delta\ln P_0 & ; \quad q_j \leq q < q_{j+1} \\ 0 & ; \quad \text{otherwise}\end{cases}$$

Measurement of kernel

- initial power spectrum $P_0(k)$: ΛCDM by wmap5
- initial perturbation ($\Delta \ln P_0$) : 1% of $P_0(k)$
- divide k=0.006~0.12 [h/Mpc] into logarithmic15 (or 13)-bins :

initial k-bin : $q_1 = 0.006\, h\,\mathrm{Mpc}^{-1}\,(\mathrm{or}\ q_1 = 0.012\, h\,\mathrm{Mpc}^{-1})$

width of k-bin : $\Delta \ln q = \ln(\sqrt{2})$

Table 1
Simulation parameters. Box size (box), softening scale (soft) and mass of the particles (mass) are respectively given in unit of h^{-1} Mpc, h^{-1} kpc and $10^{10} h^{-1} M_\odot$. The number of q-bins is shown in the "bins" column, for each of which we run two simulations with positive and negative perturbations in the linear spectrum. The "runs" column shows the number of independent initial random phases over which we repeat the same analysis. The total number of simulations are shown in the "total" column.

name	box	particles	$z_{\rm start}$	soft	mass	bins	runs	total
L9-N10	512	1024^3	63	25	0.97	5	1	10
L9-N9	512	512^3	31	50	7.74	15	4	120
L9-N8	512	256^3	15	100	61.95	13	4	104
L10-N9	1024	512^3	15	100	61.95	15	1	30
high_ns	512	512^3	31	50	7.74	5	4	40
low_ns	512	512^3	31	50	7.74	5	4	40

Run many simulations…

T.Nishimishi

Measurement results

Nishimichi, Bernardeau & AT ('16)

Response of power spectrum at k to a small initial variation at q

$$K(k,q;z) = q\frac{\delta P^{\rm nl}(k;z)}{\delta P^{\rm lin}(q;z)}$$

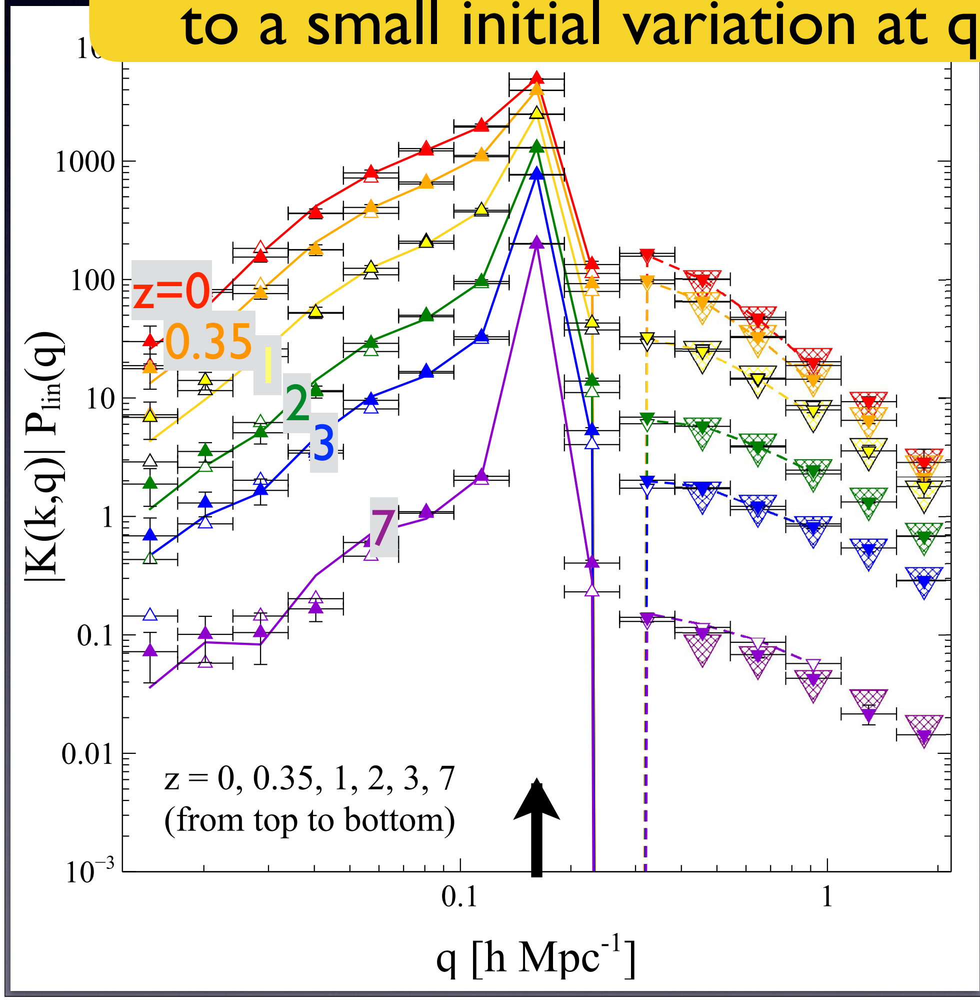

Measured at
k=0.162 [h/Mpc]

▲ or —— : positive

▼ or ------- : negative

Comparison with PT prediction

Nishimichi, Bernardeau & AT ('16)

Response of power spectrum at k to a small initial variation at q

$$K(k,q;z) = q\,\frac{\delta P^{\rm nl}(k;z)}{\delta P^{\rm lin}(q;z)}$$

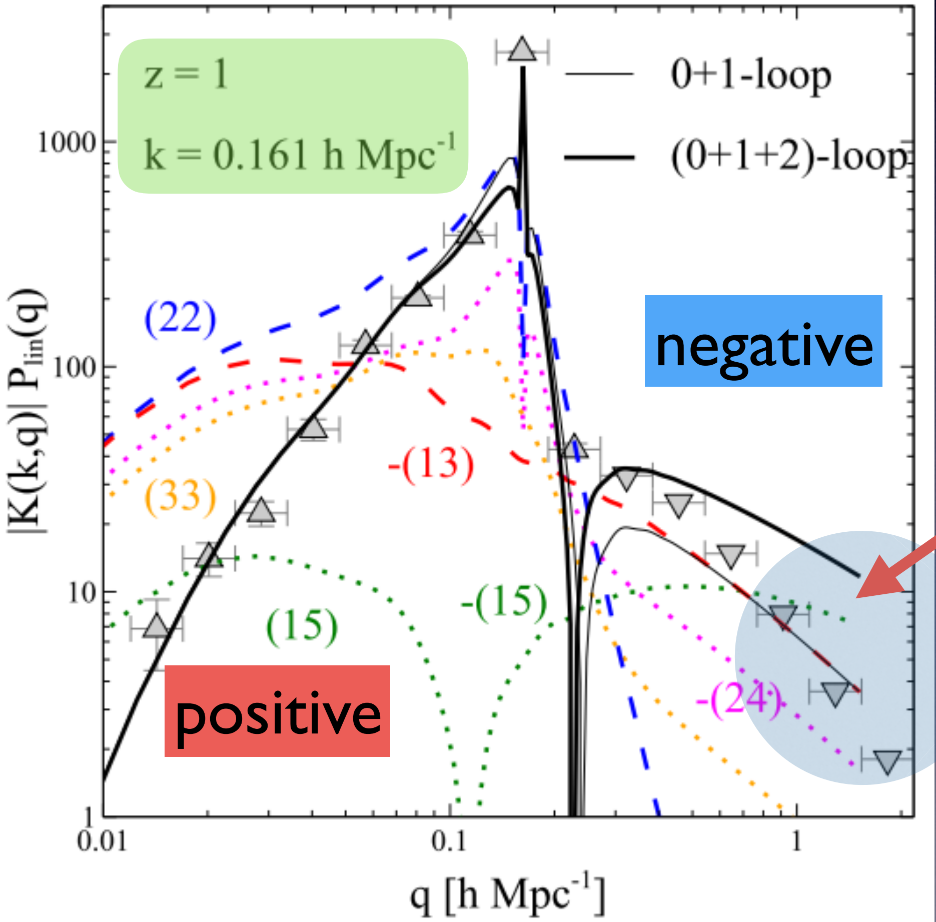

Even for *low-k* modes,

Standard PT gets a *large UV contribution* *(q-modes)*:

2-loop > 1-loop > N-body

In other words,

low-k mode in simulation is *UV-insensitive*

protected against small-scale uncertainty

Comparison with PT prediction

Nishimichi, Bernardeau & AT ('16)

Response of power spectrum at k to a small initial variation at q

$$K(k,q;z) = q\,\frac{\delta P^{\rm nl}(k;z)}{\delta P^{\rm lin}(q;z)}$$

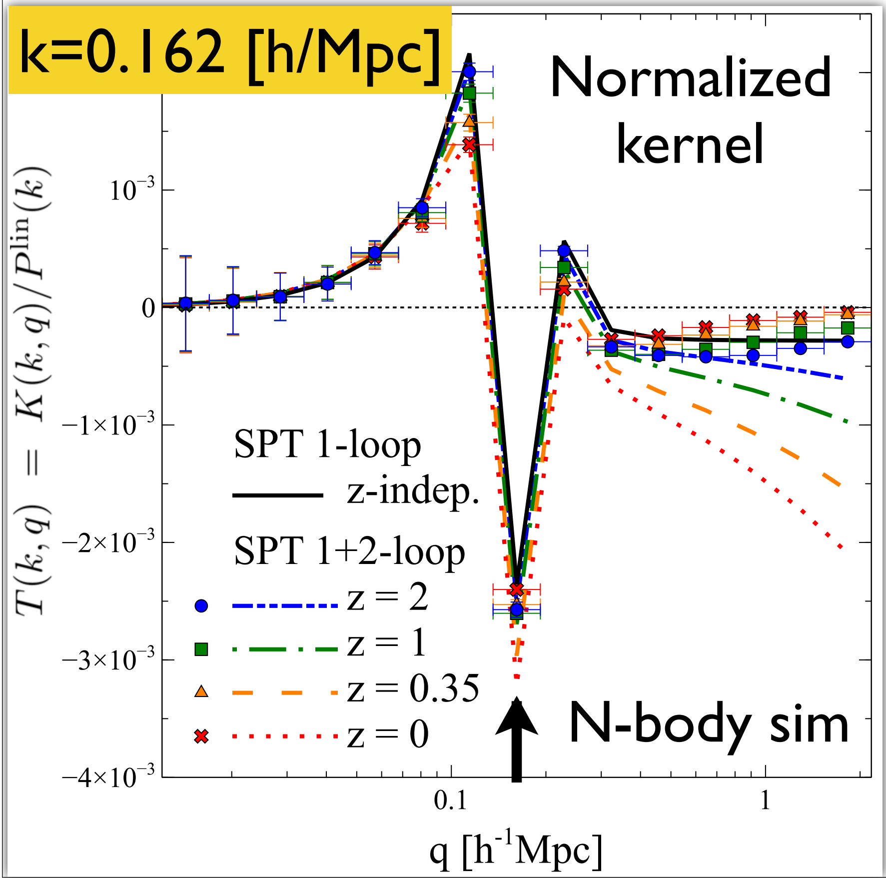

Black solid : Standard PT 1-loop (z-indept.)

Blue Green Orange Red

q<k : reproduce simulation well

q>k : discrepancy is manifest (particularly large at low-z)

UV contribution is suppressed !!

Refined measurement

Nishimichi, Bernardeau & AT ('16 &'17 in prep.)

Response of power spectrum at k to a small initial variation at q

$$K(k,q;\,z) = q\frac{\delta P_{\rm nl}(k;\,z)}{\delta P_0(q;\,z)}$$

1,400 simulations

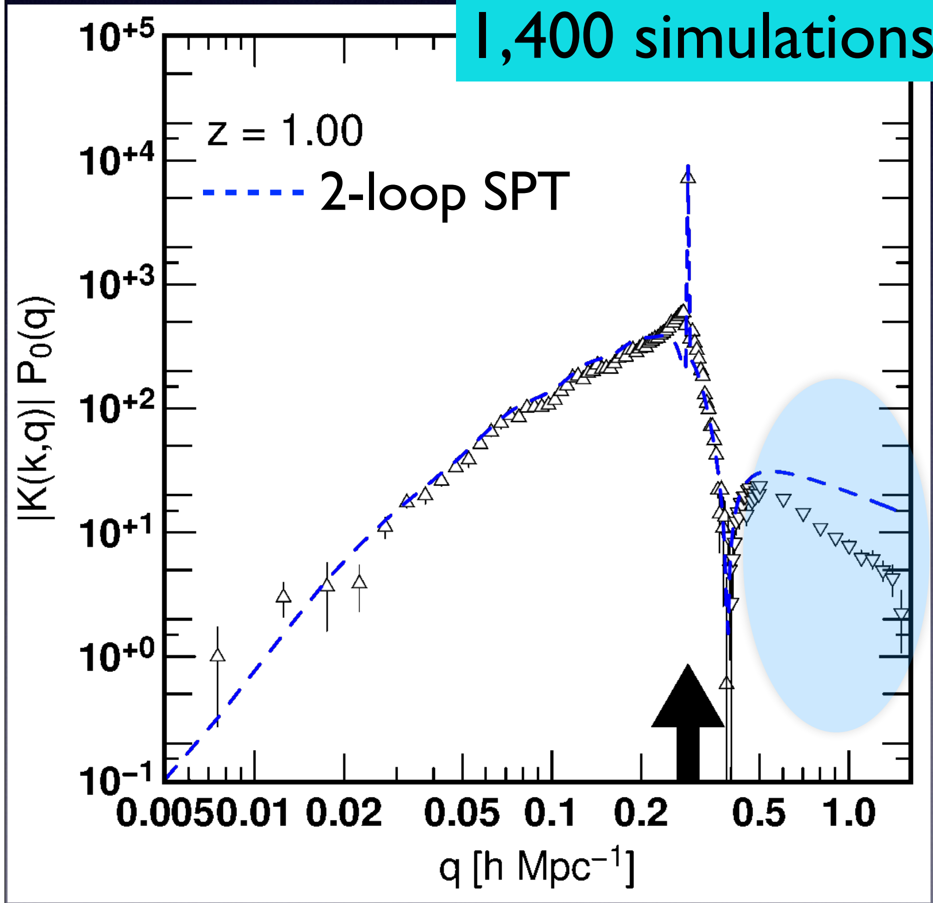

$$T(k,q) = [K(k,q) - K^{\rm lin}(k,q)]/[qP^{\rm lin}(k)]$$

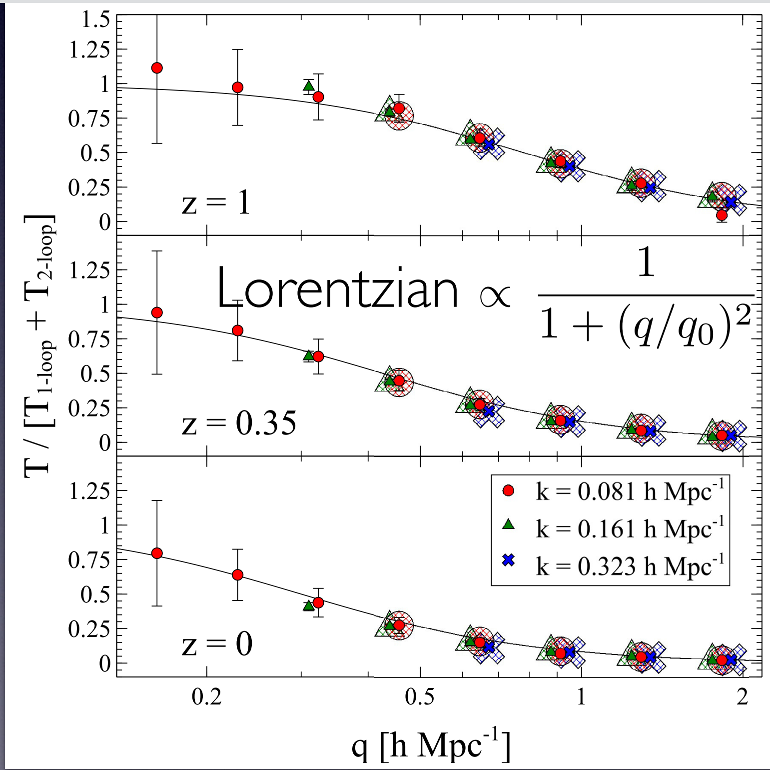

UV suppression is seen at various k

Refined measurement

Nishimichi, Bernardeau & AT ('16 &'17 in prep.)

Response of power spectrum at k to a small initial variation at q

$$K(k,q;\,z) = q\frac{\delta P_{\rm nl}(k;\,z)}{\delta P_0(q;\,z)}$$

1,400 simulations

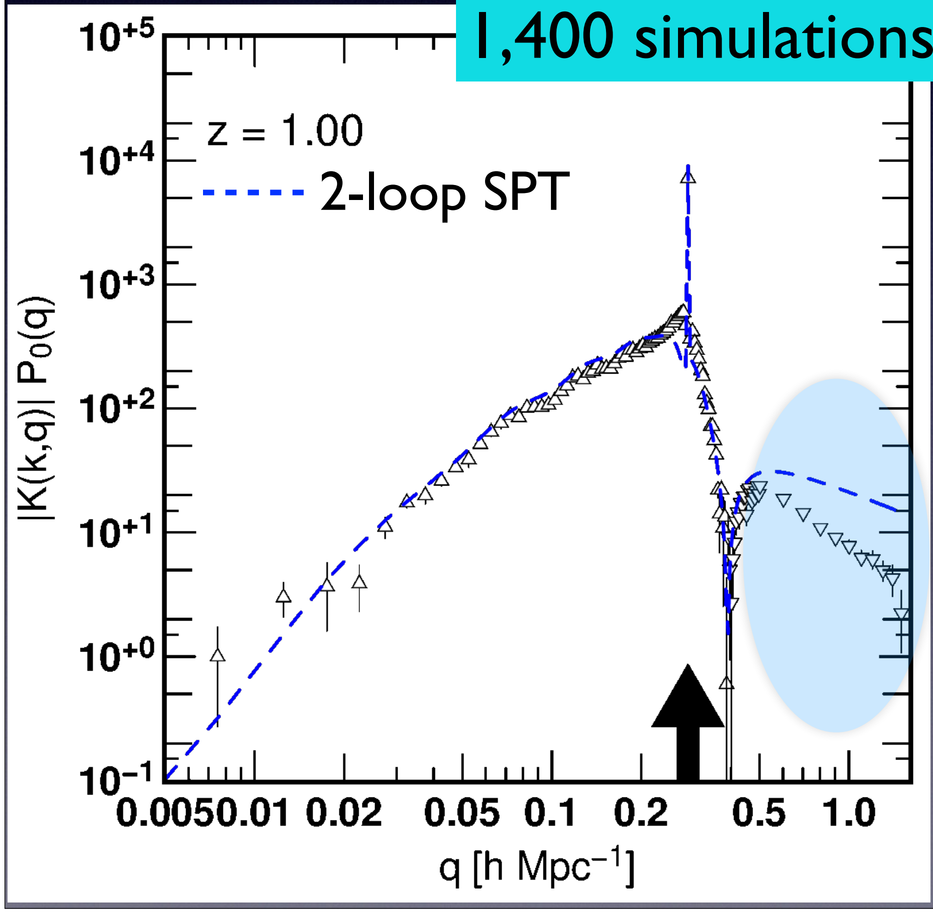

$$T(k,q) = [K(k,q) - K^{\rm lin}(k,q)]/[qP^{\rm lin}(k)]$$

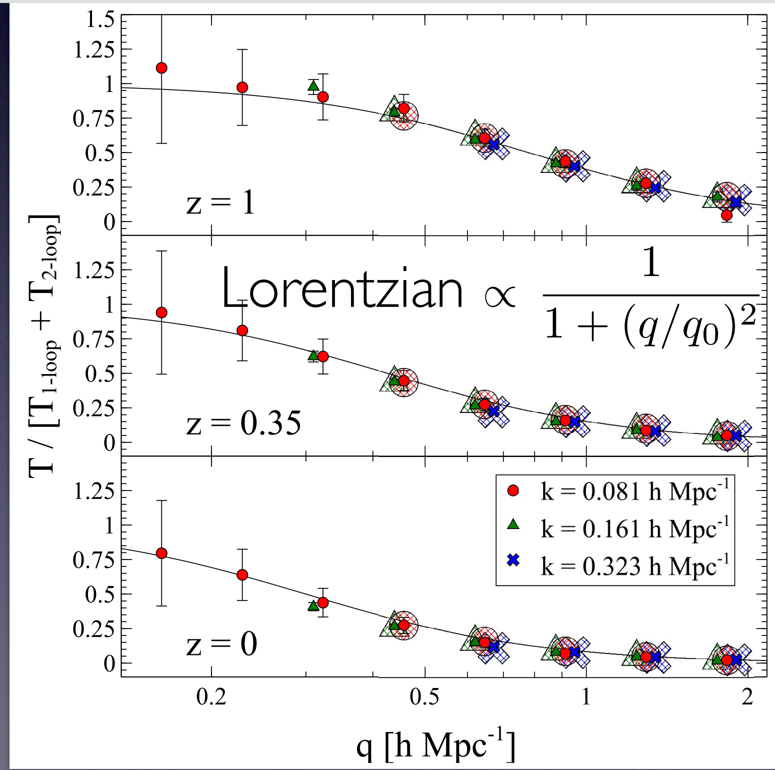

UV suppression is seen at various k

Reconstructing nonlinear P(k)

simulation — Response funcion

$$P_{\rm target}(k) = P_{\rm fiducial}(k) + \int d\ln q\, \underbrace{K(k,q)}_{\textit{w/ damping}} \{\underbrace{P_{0,\rm target}(q) - P_{0,\rm fiducial}(q)}_{\text{Linear power spectrum}}\}$$

fiducial: Planck 15
target: wmap3

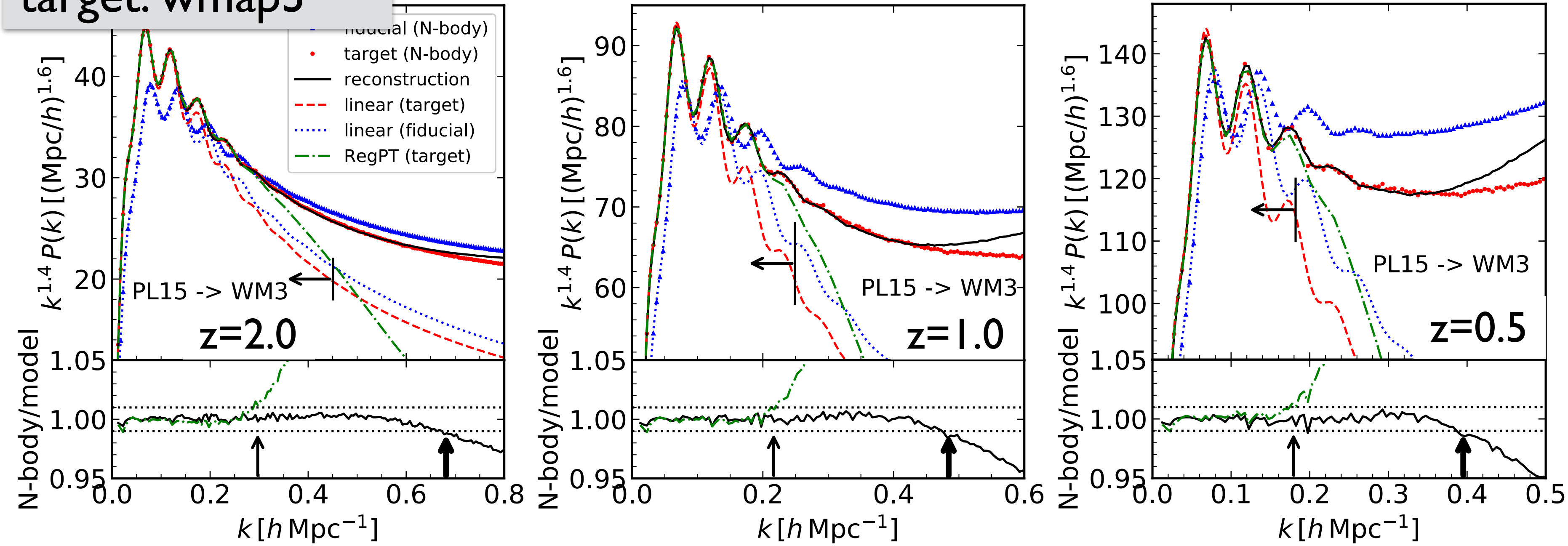

Nishimichi et al. (in prep)

Response func. with damping gives a better agreement with simulation

Summary

- Higher-order mode-coupling gets a larger UV contribution

Blas, Garny & Konstandin ('14), Bernardeau, AT & Nishimichi ('14)

However

- In simulation, actual UV contribution is suppressed

Nishimichi, Bernardeau & AT ('16, '17 in prep.)

Breakdown of single-stream PT treatment can be seen even at large scales

What is a role of <u>small-scale dynamics ?</u>

Is there a way to go beyond single-stream PT ?

Multi-stream flows

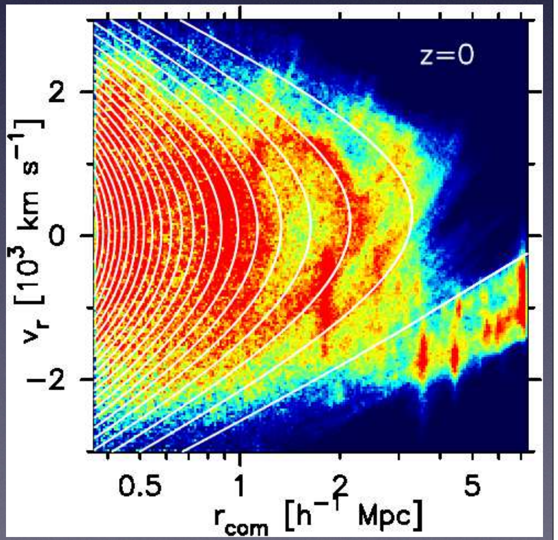

Suto et al. (2016)

Beyond single-stream approx.: lesson from 1D cosmology

AT & Colombi, arXiv:1701.09088

Vlasov-Poisson: back to the source

A more fundamental description :

Vlasov-Poisson system

(collisionless Boltzmann)

$$\left[a\frac{\partial}{\partial t} + \frac{\boldsymbol{v}}{a}\cdot\frac{\partial}{\partial \boldsymbol{x}} - a\frac{\partial \phi}{\partial \boldsymbol{x}}\cdot\frac{\partial}{\partial \boldsymbol{v}} \right] f(\boldsymbol{x},\,\boldsymbol{v};\,t) = 0$$

$$\nabla^2\phi(x;\,t) = 4\pi\, G\, a^2 \int d^3\boldsymbol{v}\, f(\boldsymbol{x},\,\boldsymbol{v};\,t)$$

- N→∞ limit of self-gravitating N-body system
- Reduced to a (pressureless) fluid system for *single-stream flow*:

$$f(\boldsymbol{x},\,\boldsymbol{v};\,t) \to \overline{\rho}(t)\,\{1+\delta(\boldsymbol{x};\,t)\}\,\delta_{\rm D}\left(\boldsymbol{v}-\boldsymbol{v}(\boldsymbol{x};\,t)\right)$$

Single-stream flow is initially correct, but will be later violated

(at small scales)

Vlasov-Poisson: back to the source

A more fundamental description :

Vlasov-Poisson system

(collisionless Boltzmann)

$$\left[a \frac{\partial}{\partial t} + \frac{\boldsymbol{v}}{a} \cdot \frac{\partial}{\partial \boldsymbol{x}} - a \frac{\partial \phi}{\partial \boldsymbol{x}} \cdot \frac{\partial}{\partial \boldsymbol{v}} \right] f(\boldsymbol{x}, \boldsymbol{v}; t) = 0$$

$$\nabla^2 \phi(x; t) = 4\pi G a^2 \int d^3\boldsymbol{v}\, f(\boldsymbol{x}, \boldsymbol{v}; t)$$

cannot be described by fluid-based PT treatment

<u>Cold collapse in 1D gravity (simulation)</u>

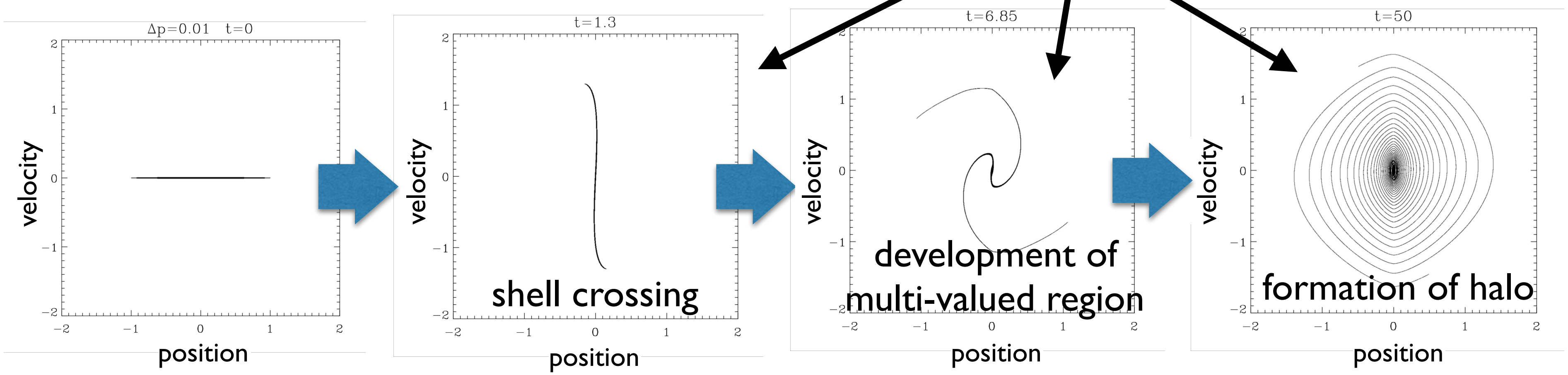

Vlasov-Poisson: back to the source

A more fundamental description :

Vlasov-Poisson system

(collisionless Boltzmann)

$$\left[a\frac{\partial}{\partial t} + \frac{\boldsymbol{v}}{} \cdot \frac{\partial}{\partial} - a\frac{\partial\phi}{\partial} \cdot \frac{\partial}{\partial} \right] f(\boldsymbol{x},\, \boldsymbol{v};\, t) = 0$$

$$\nabla^2$$

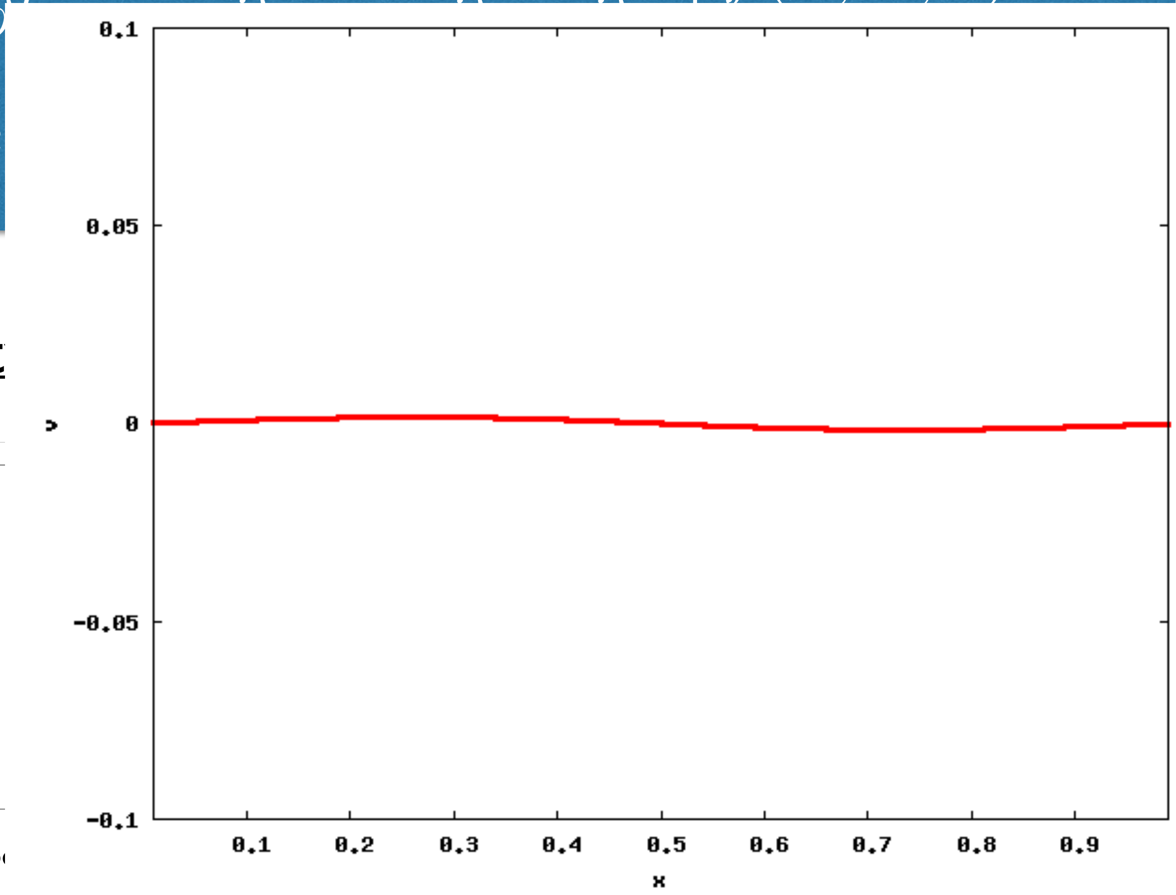

Cold collapse in 1D gravit

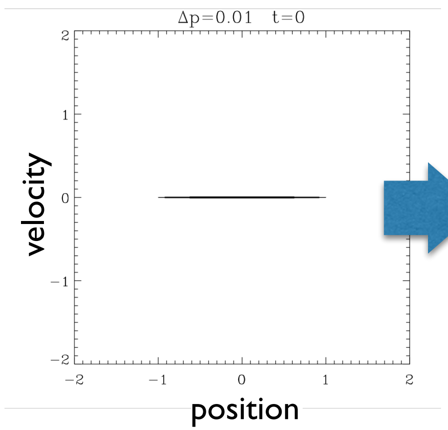

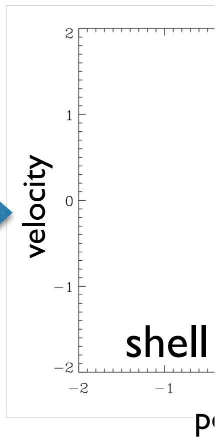

1D cosmology

Simplification may help us to understand what's going on

$$\nabla_x^2\phi(x) = 4\pi\, G\overline{\rho}\, a^2\, \delta(x)$$

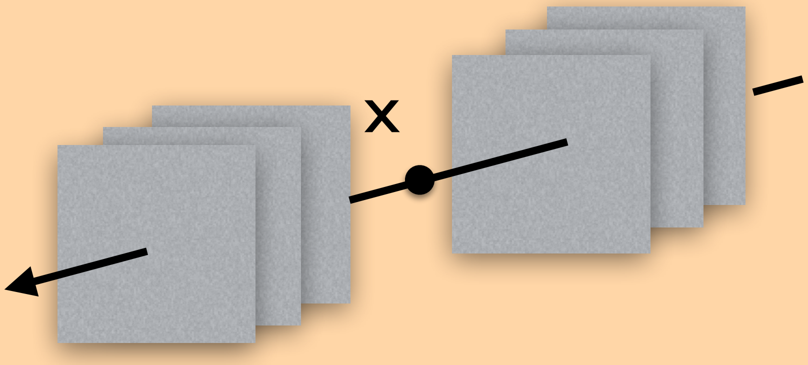

Force $\propto$ (# of sheets at RHS) - (# of sheets at LHS)

- Generic features of nonlinear mode-coupling :

  Response function

- Perturbative description beyond shell-crossing: Post-collapse PT

Learn something in simple *1D cosmology*

1D Zel'dovich solution

(Zel'dovich '70)

Exact single-stream solution

$$x(q;\tau) = q + \psi(q)\, D_+(\tau)$$

$$\mathrm{v}(q;\tau) = \psi(q)\, \frac{dD_+(\tau)}{d\tau}$$

$D_+(\tau)$: linear growth factor

$\psi(q)$: displacement field

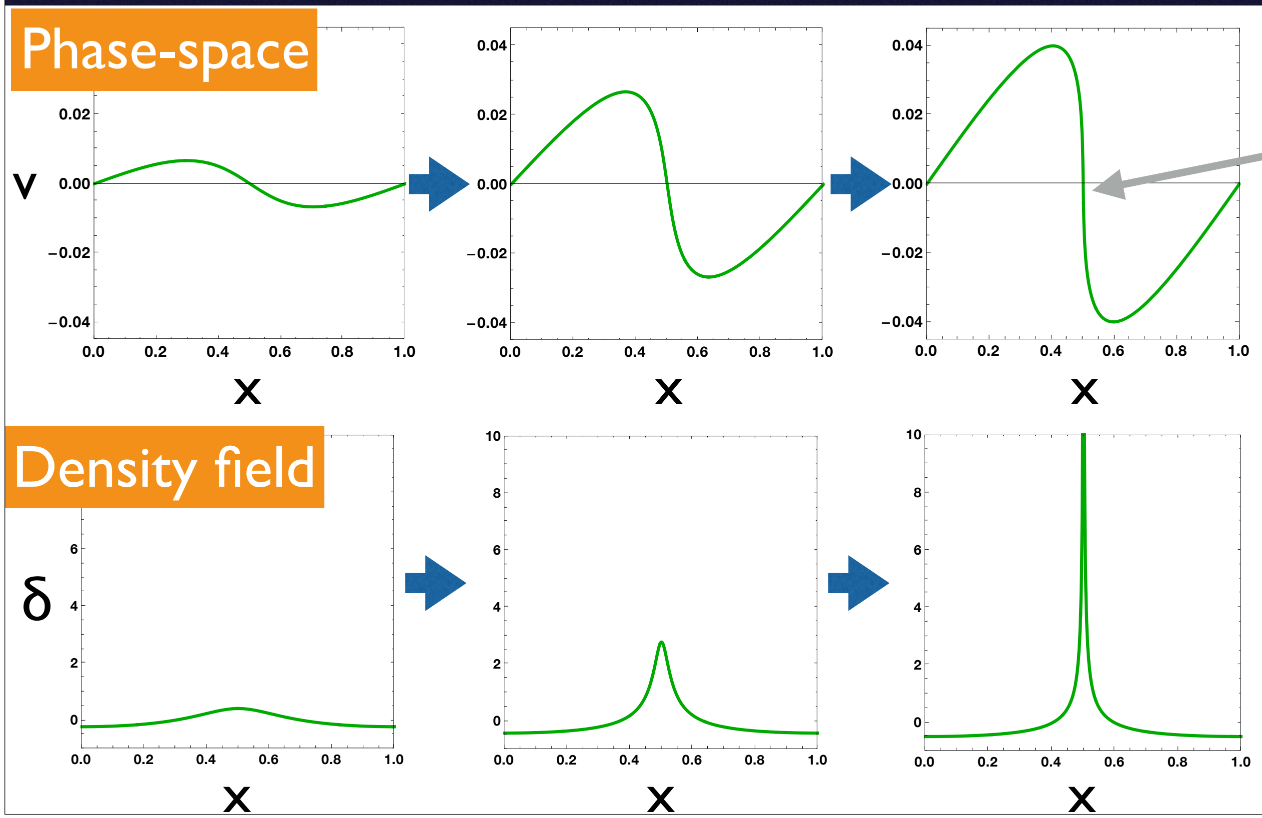

Shell crossing

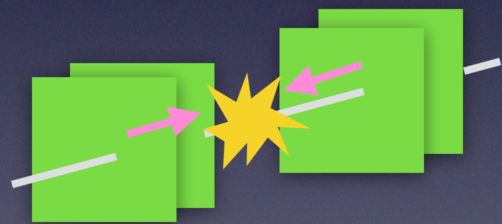

Solution is exact until shell crossing

Power spectrum in 1D

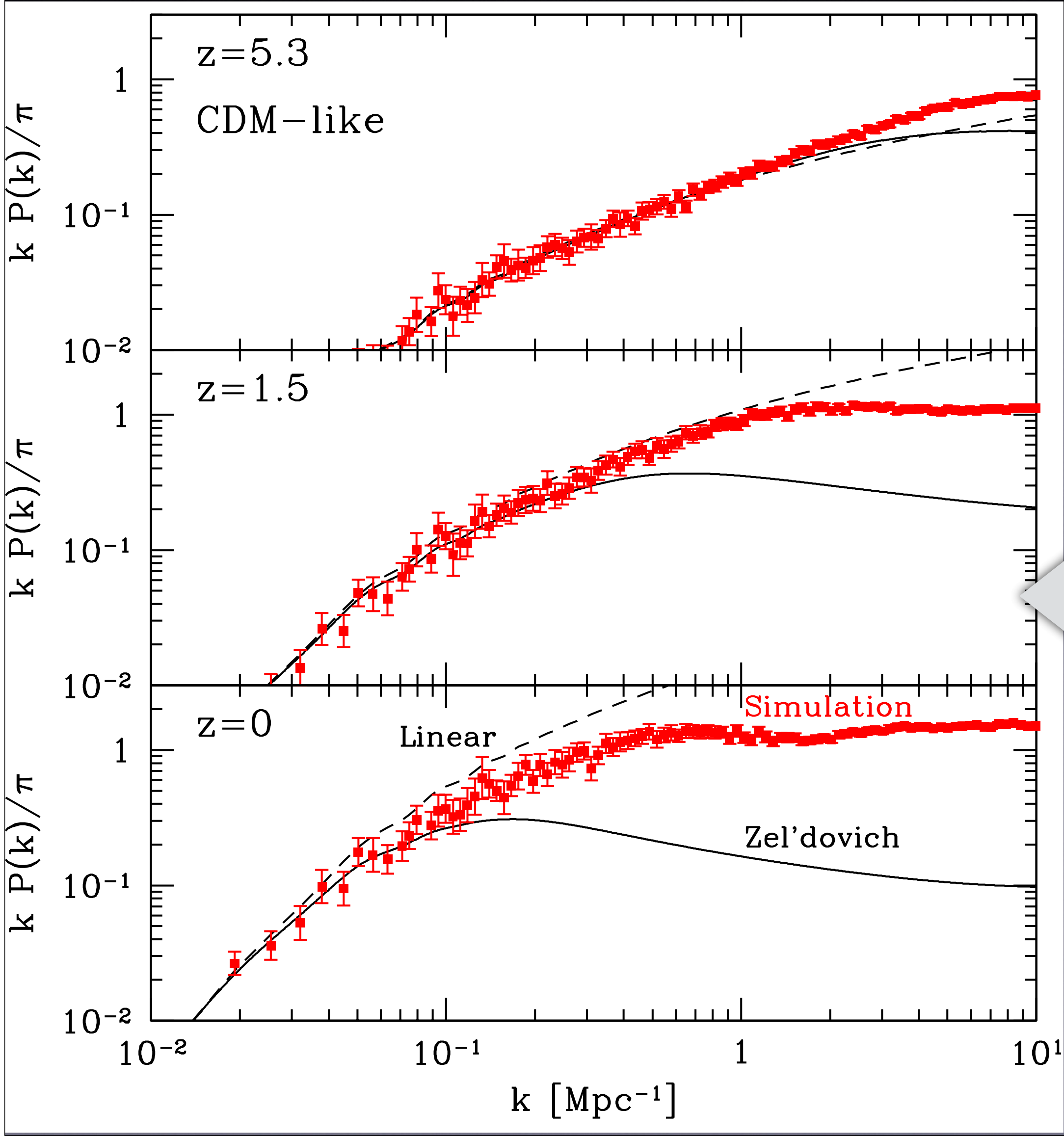

Initial Planck ΛCDM

$$P_{1\mathrm{D}}(k) = \frac{k^2}{2\pi} P_{3\mathrm{D}}(k)$$

Dimensionless initial power spectrum is the same as in 3D

manifestation of the limitation of single-stream treatment

$L = 1,000\,\mathrm{Mpc}$
\# of particles (sheets) : $200,000$
\# of runs : 50

by Vlafroid (PM code)

http://www.vlasix.org/uploads/Main/froid1D.1.5.tar.gz w/ A. Halle, S. Colombi & T. Nishimichi (in progress)

Response function in 1D

$$K(k,q;\,z) = q\,\frac{\delta P_{\rm nl}(k;\,z)}{\delta P_0(q;\,z)}$$

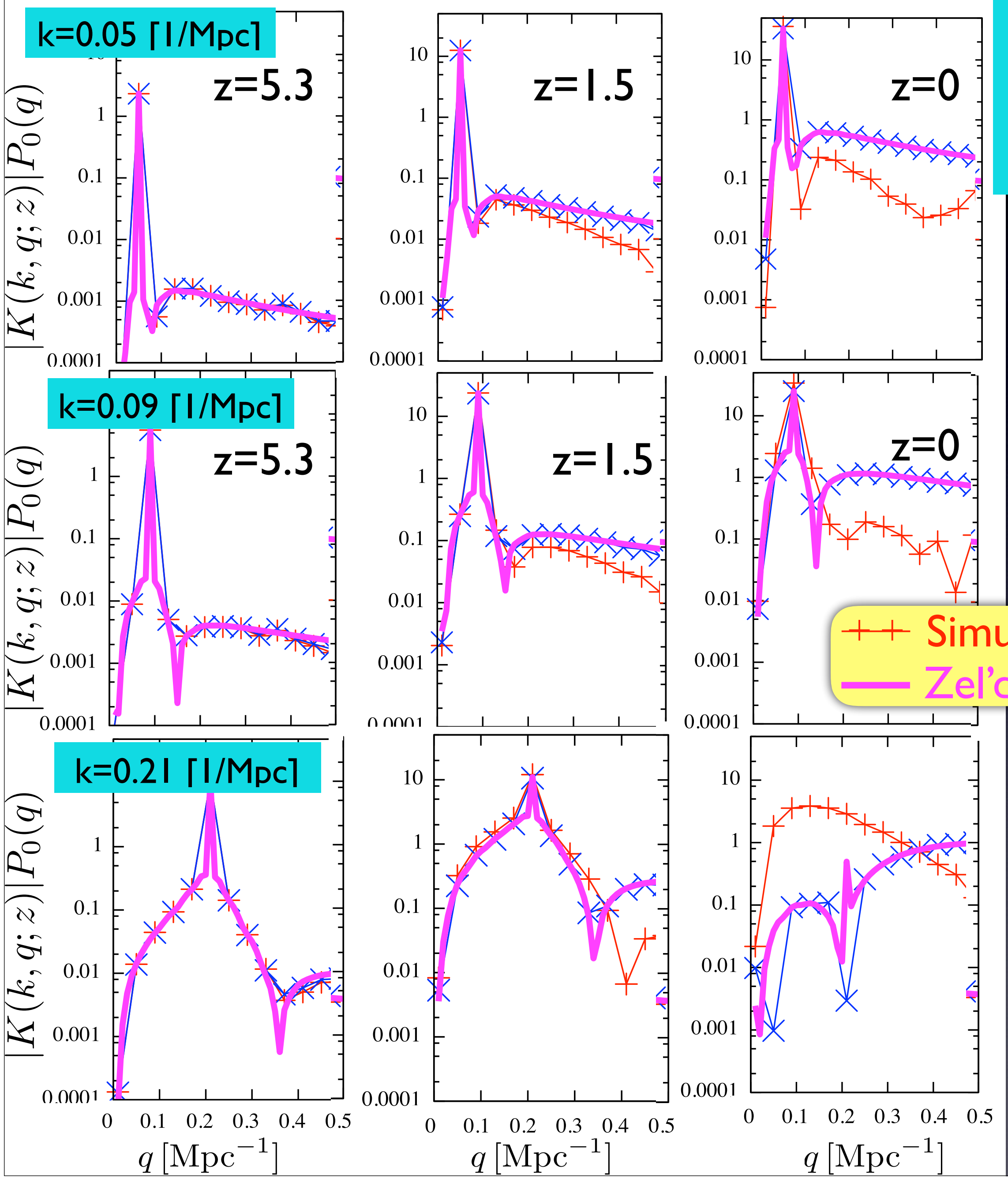

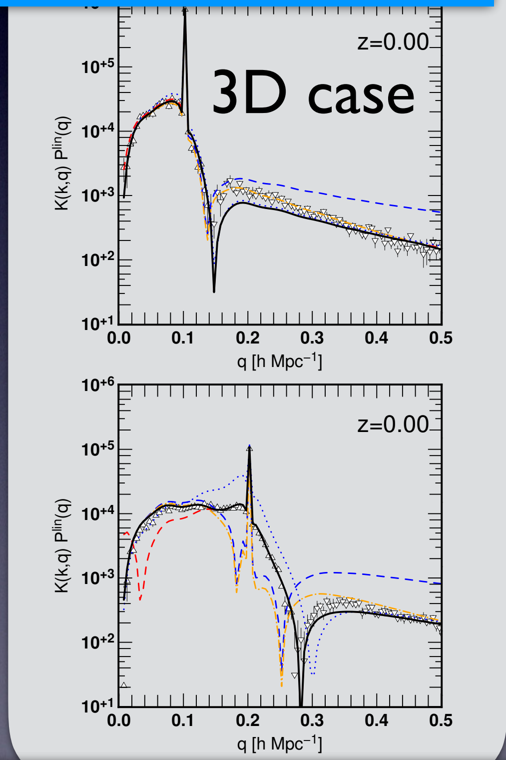

$L = 100,000\mathrm{Mpc}$
\# of particles (sheets) : 10^7
\# of runs : $2,000$ for each q-mode

Post-collapse PT: beyond shell-crossing

AT & Colombi ('17)

Cold collapse in 1-D simulation

Breakdown of Zel'dovich solution

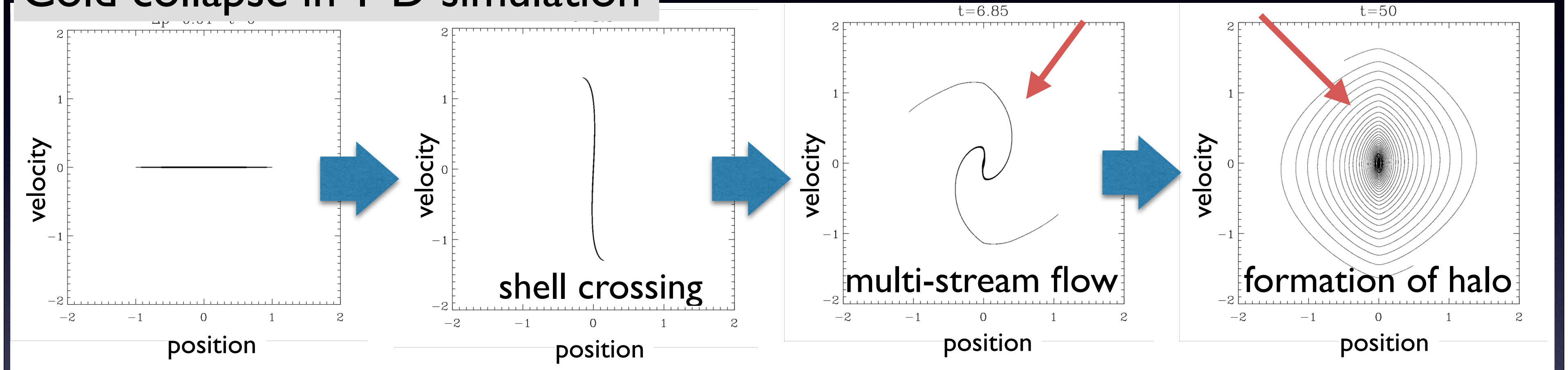

Computing back-reaction to the Zel'dovich flow: *Lagrangian*

1. Expand the displacement field around *shell-crossing point*, q_0:

$$x(q;\tau) \simeq A(q_0;\tau) - B(q_0;\tau)(q-q_0) + C(q_0;\tau)(q-q_0)^3$$

2. Compute force $F(x(q;\tau)) = -\nabla_x \Phi(x(q;\tau))$ at multi-stream region

$$\Delta \mathrm{v}(Q;\tau,\tau_\mathrm{q}) = \int_{\tau_\mathrm{q}}^{\tau} d\tau'\, F(x(Q,\tau')), \quad \Delta x(Q;\tau,\tau_\mathrm{q}) = \int_{\tau_\mathrm{q}}^{\tau} d\tau'\, \Delta \mathrm{v}(Q;\tau',\tau_\mathrm{q})$$

...... polynomial function of *Q=q-q0 up to 7th order*

Post-collapse PT: single cluster

AT & Colombi ('17)

Post-collapse PT basically fails after next shell-crossing, but it still gives reasonable prediction for density profiles

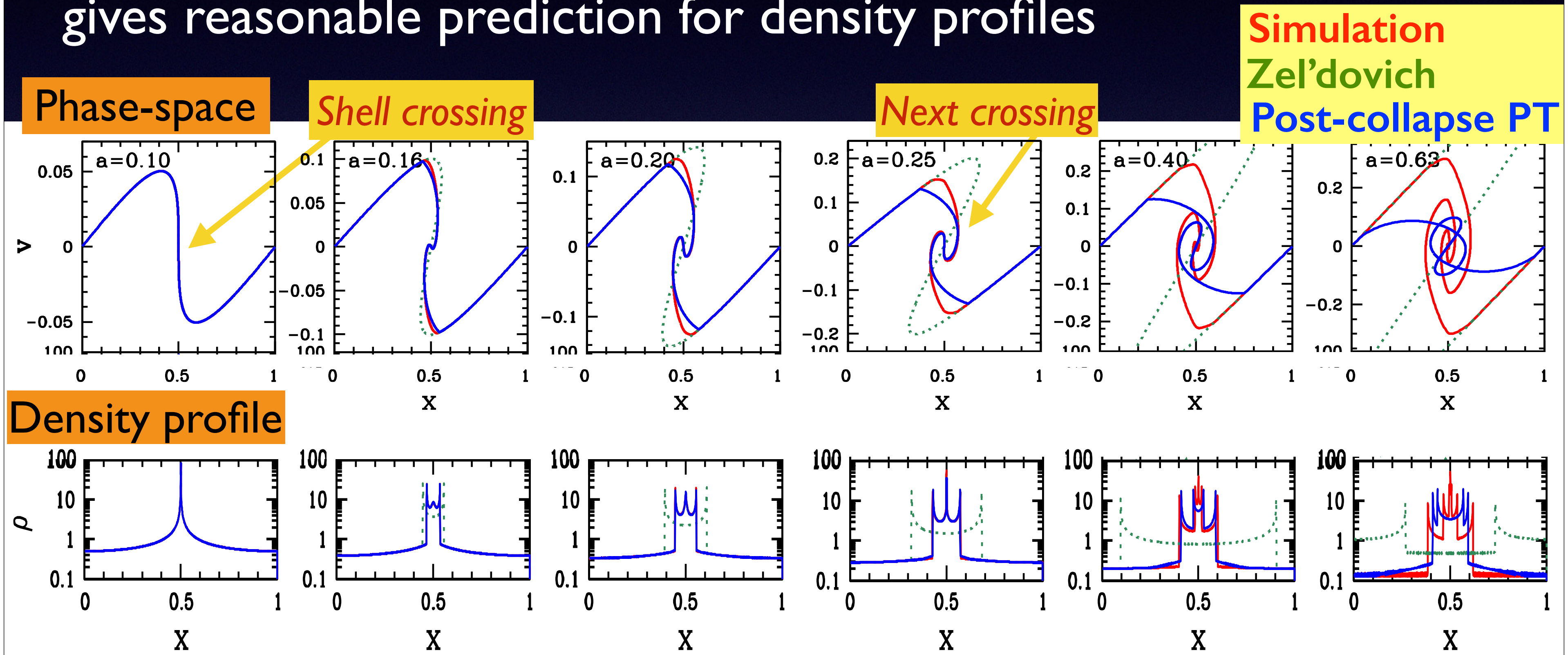

Of course, this does not guarantee the accuracy of power spectrum prediction at small scales (→ next slide)

Post-collapse PT: ΛCDM

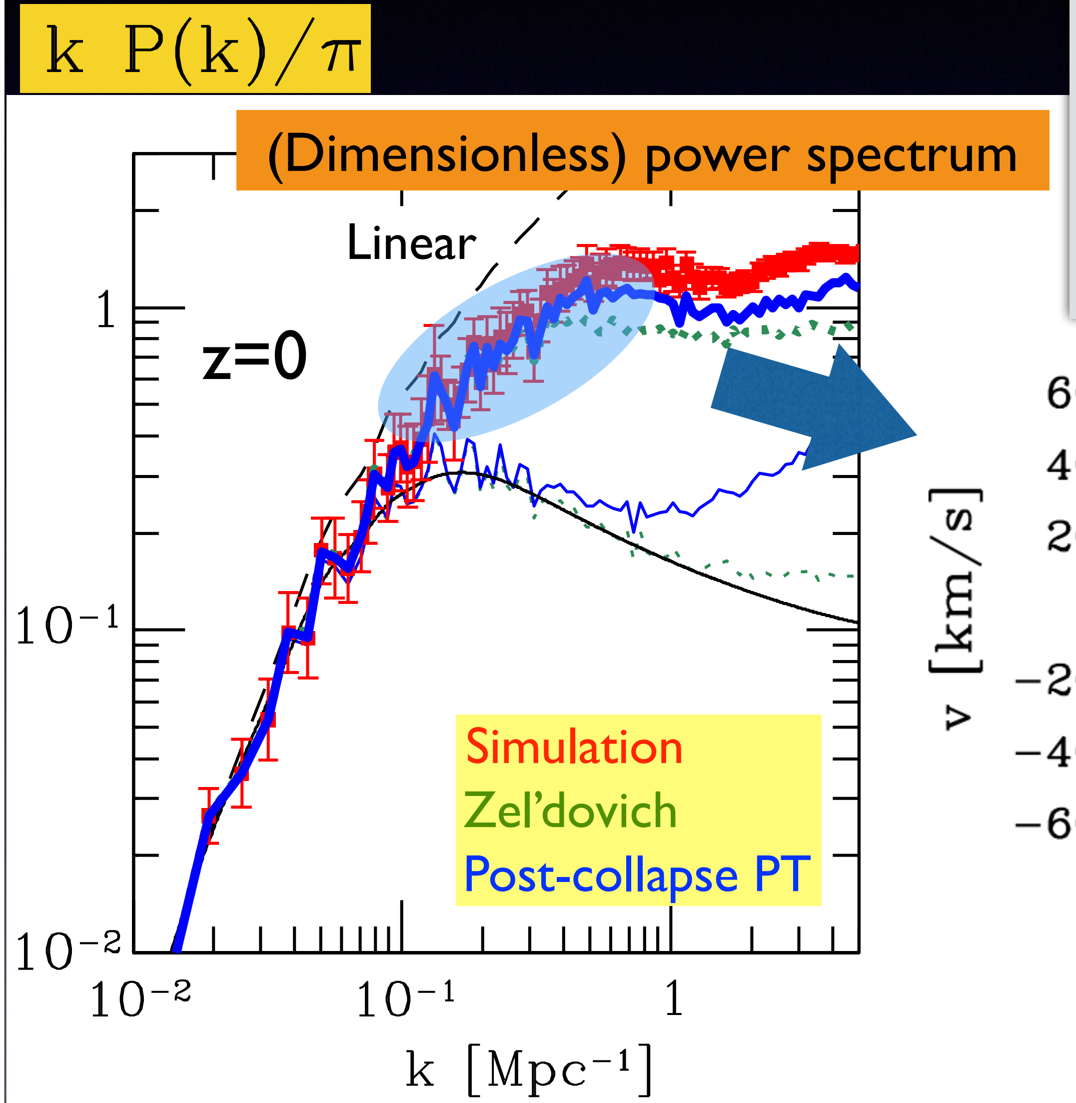

Adaptive smoothing
applied to initial density peaks
(with filter scales determined
by first-barrier crossing)

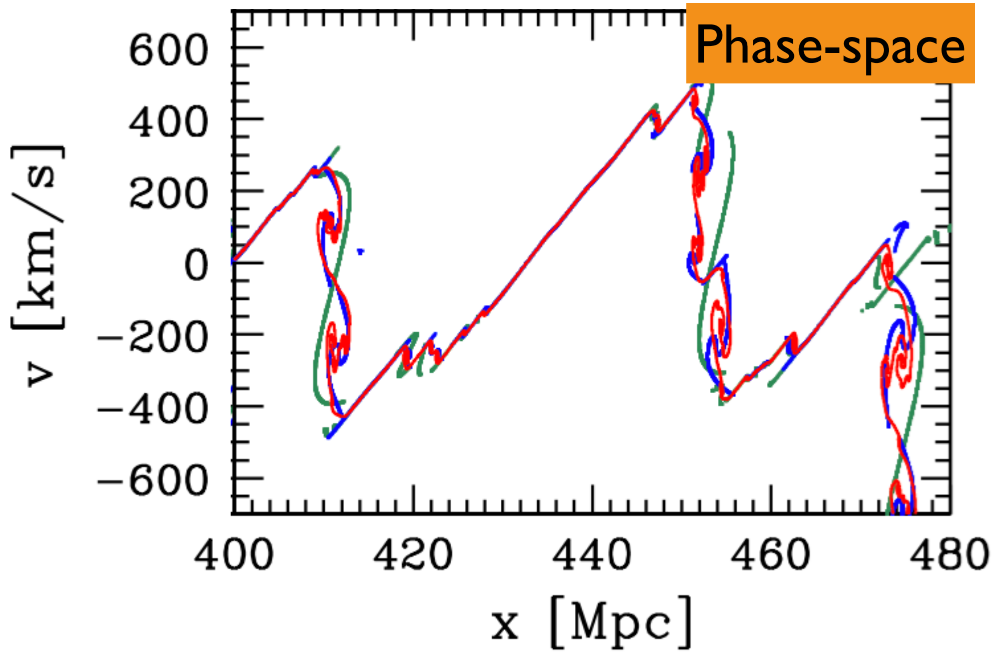

AT & Colombi ('17)

Implication to 3D

Combination of the two methods are rather crucial:

PT scheme beyond shell crossing & *Coarse-graining*

(post-collapse PT) *(adaptive smoothing)*

But, idea & technique are very promising and can be extended to 3D

Issues to be addressed

- Accurate pre-collapse description
  - ✓ Zel'dovich approx. is inaccurate
  - ✓ Various topologies of shell crossing
- Tractable analytical calculation of statistical quantities

2D collapse with Vlasov code

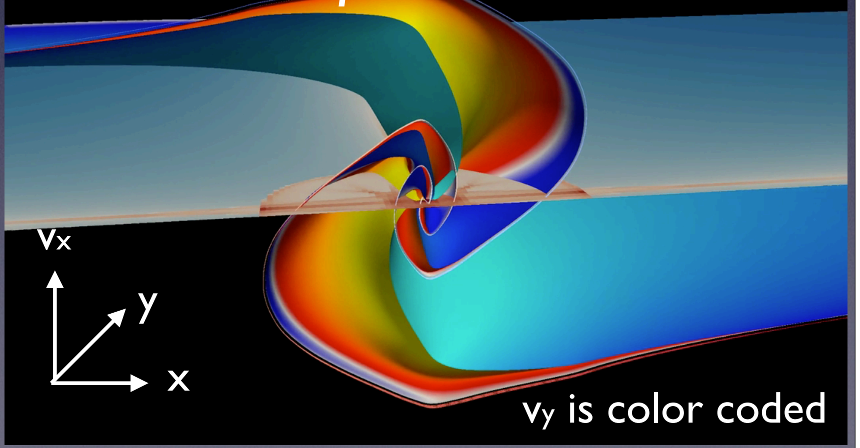

http://www.vlasix.org/index.php?n=Main.ColDICE

Implication to 3D

Combination of the two methods are rather crucial:

PT scheme beyond shell crossing & *Coarse-graining*

(post-collapse PT) *(adaptive smoothing)*

But, idea & technique are very promising and can be extended to 3D

Issues to be addressed

- Accurate pre-collapse description
  - ✓ Zel'dovich approx. is inaccurate
  - ✓ Various topologies of shell crossing
- Tractable analytical calculation of statistical quantities

2D collapse with Vlasov code

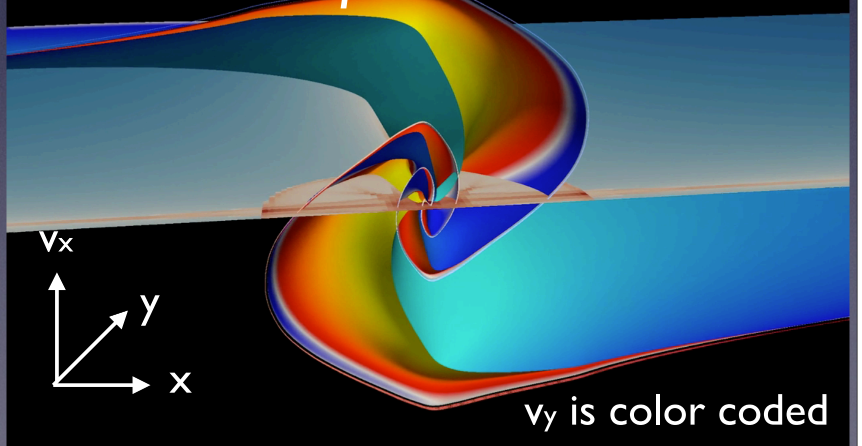

http://www.vlasix.org/index.php?n=Main.ColDICE

Implication to 3D

Combination of the two methods are rather crucial:

PT scheme beyond shell crossing & *Coarse-graining*

(post-collapse PT) *(adaptive smoothing)*

But, idea & technique are very promising and can be extended to 3D

Issues to be addressed

- Accurate pre-collapse description
  - ✓ Zel'dovich approx. is inaccurate
  - ✓ Various topologies of shell crossing
- Tractable analytical calculation of statistical quantities

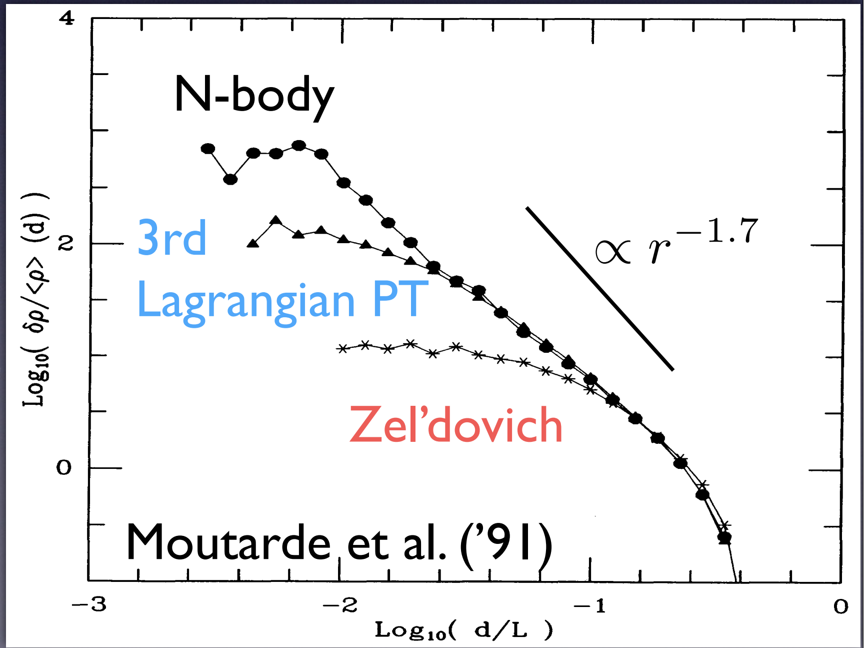

State-of-the-art cosmological Vlasov code

DIRECT INTEGRATION OF THE COLLISIONLESS BOLTZMANN EQUATION IN SIX-DIMENSIONAL PHASE SPACE: SELF-GRAVITATING SYSTEMS

2013

Kohji Yoshikawa[1], Naoki Yoshida[2,3], and Masayuki Umemura[1]
[1] Center for Computational Sciences, University of Tsukuba, 1-1-1 Tennodai, Tsukuba, Ibaraki 305–8577, Japan;
[2] Department of Physics, The University of Tokyo, Tokyo 113-0033, Japan
[3] Kavli Institute for the Physics and Mathematics of the Universe, The University of Tokyo, Kashiwa, Chiba 277-8583, Japan

Received 2012 June 18; accepted 2012 November 23; published 2012 December 20

64^6

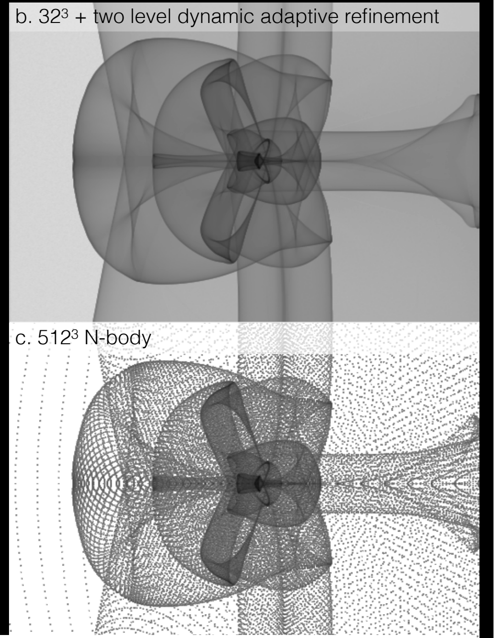

An adaptively refined phase-space element method for cosmological simulations and collisionless dynamics

Oliver Hahn[⋆1] and Raul E. Angulo[†2]
[1] *Department of Physics, ETH Zurich, CH-8093 Zürich, Switzerland*
[2] *Centro de Estudios de Física del Cosmos de Aragón, Plaza San Juan 1, Planta-2, 44001, Teruel, Spain.*

Cold initial condition

2016

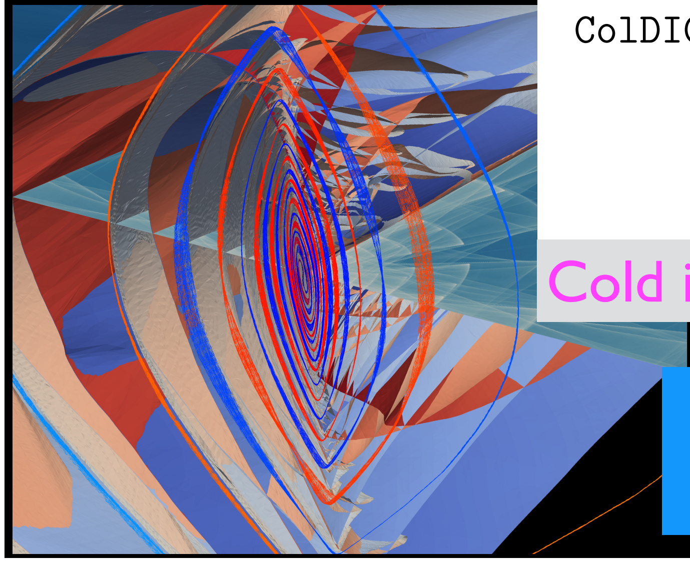

`ColDICE`: a parallel Vlasov-Poisson solver using moving adaptive simplicial tessellation

2016

Thierry Sousbie[a,b,c,*], Stéphane Colombi[a]
[a] *Institut d'Astrophysique de Paris, CNRS UMR 7095 and UPMC, 98bis, bd Arago, F-75014 Paris, France*
...sics, The University of Tokyo, Tokyo 113-0033, Japan
...rse, School of Science, The University of Tokyo, Tokyo 113-0033, Japan

Cold initial condition

Analytic treatment helps to understand Vlasov simulations

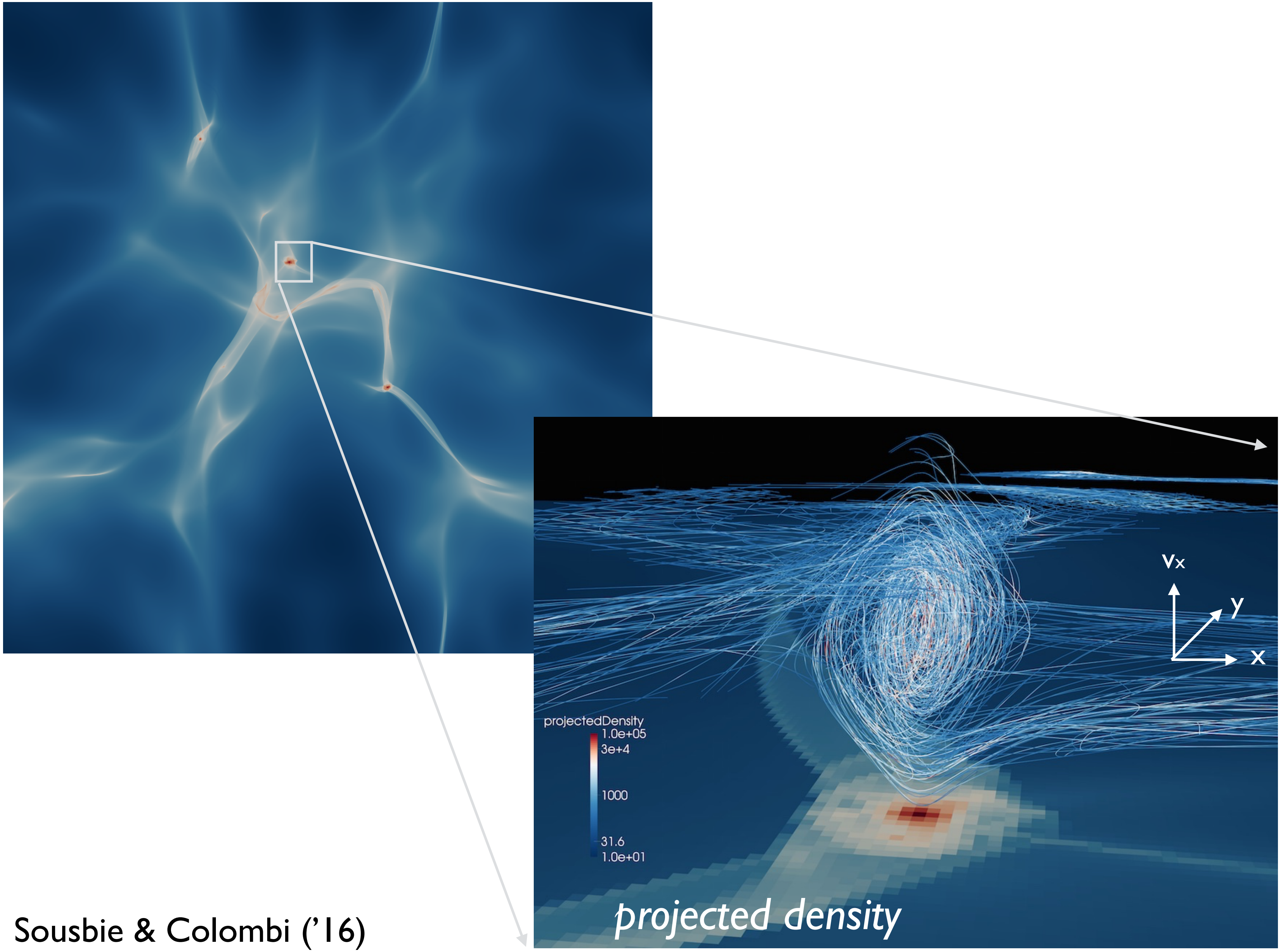

Sousbie & Colombi ('16)

Describing shell-crossing in 3D

Motivation

- Post-collapse PT treatment needs an accurate analytical description of shell-crossing structure
- In 3D, Zel'dovich solution is no longer exact even before shell-crossing

In a specific initial condition,

✓ Higher-order Lagrangian PT

✓ Comparison with 6D Vlasov simulation

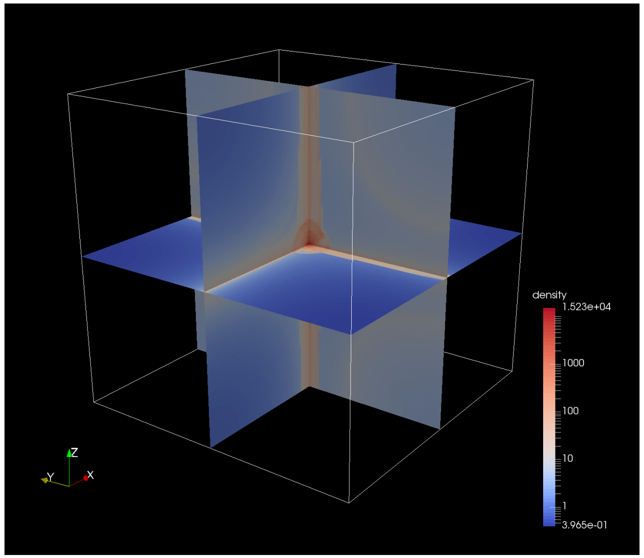

Lagrangian PT

Basic equations

$$L = \frac{1}{2}\, m\, a^2 \dot{\boldsymbol{x}}^2 - m\,\phi(\boldsymbol{x})$$

$$\ddot{\boldsymbol{x}} + 2H\dot{x} = -\frac{1}{a^2}\,\nabla_x\,\phi(\boldsymbol{x}),$$
$$\nabla_x^2\,\phi(\boldsymbol{x}) = 4\pi\,Ga^2\overline{\rho}_{\rm m}\,\delta(\boldsymbol{x}).$$

Lagrangian coordinate (***q***): $\boldsymbol{x}(\boldsymbol{q},t) = \boldsymbol{q} + \boldsymbol{\Psi}(\boldsymbol{q},t)$

In Lagrangian coordinate, mass density is assumed to be uniform:

$$\overline{\rho}_{\rm m}\,d^n\boldsymbol{q} = \rho_{\rm m}(\boldsymbol{x})\,d^n\boldsymbol{x} \longrightarrow \delta(\boldsymbol{x}) = \frac{\rho_{\rm m}(\boldsymbol{x})}{\overline{\rho}_{\rm m}} - 1 = \left|\frac{\partial \boldsymbol{x}}{\partial \boldsymbol{q}}\right|^{-1} - 1$$

Rewriting quantities in Eulerian space with those in Lagrangian quantities

Lagrangian PT

Matsubara ('15)

$$\nabla_x \cdot \left[\ddot{\boldsymbol{x}} + 2H\dot{\boldsymbol{x}}\right] = -4\pi\, G\,\overline{\rho}_{\rm m}\,\delta,$$

$$\nabla_x \times \left[\ddot{\boldsymbol{x}} + 2H\dot{\boldsymbol{x}}\right] = \boldsymbol{0}.$$

$$\hat{\mathcal{T}} f(t) \equiv \ddot{f}(t) + 2H\dot{f}(t)$$

Longitudinal: $\left(\hat{\mathcal{T}} - 4\pi\, G\,\overline{\rho}_{\rm m}\right)\Psi_{k,k}$

$$= -\epsilon_{ijk}\epsilon_{ipq}\,\Psi_{j,p}\left(\hat{\mathcal{T}} - 2\pi\, G\,\overline{\rho}_{\rm m}\right)\psi_{k,q}$$

$$- \frac{1}{2}\epsilon_{ijk}\epsilon_{pqr}\,\Psi_{i,p}\Psi_{j,q}\left(\hat{\mathcal{T}} - \frac{4\pi\, G}{3}\,\overline{\rho}_{\rm m}\right)\Psi_{k,r},$$

Transverse: $\epsilon_{ijk}\,\hat{\mathcal{T}}\,\Psi_{j,k} = -\epsilon_{ijk}\,\Psi_{p,j}\hat{\mathcal{T}}\Psi_{p,k}.$

Levi-Civita symbol

PT expansion: $\boldsymbol{\Psi}(\boldsymbol{q},\,t) = \boldsymbol{\Psi}^{(1)}(\boldsymbol{q},\,t) + \boldsymbol{\Psi}^{(2)}(\boldsymbol{q},\,t) + \boldsymbol{\Psi}^{(3)}(\boldsymbol{q},\,t) + \cdots$

Lagrangian PT

Matsubara ('15)

Under Einstein-de Sitter approximation: $\mathbf{\Psi}^{(n)}_{\text{EdS}}(\boldsymbol{q};\,a(t)) \longrightarrow \mathbf{\Psi}^{(n)}(\boldsymbol{q};\,D_1(t))$

$$\eta \equiv \ln D_1(t)$$

Longitudinal: $$\left(\frac{\partial^2}{\partial\eta^2}+\frac{1}{2}\frac{\partial}{\partial\eta}-\frac{3}{2}\right)\Psi^{(n)}_{k,k}$$
$$= -\sum_{m_1+m_2=n} \underline{\epsilon_{ijk}\epsilon_{ipq}\,\Psi^{(m_1)}_{j,p}\left(\frac{\partial^2}{\partial\eta^2}+\frac{1}{2}\frac{\partial}{\partial\eta}-\frac{3}{4}\right)\psi^{(m_2)}_{k,q}}$$
$$-\frac{1}{2}\sum_{m_1+m_2+m_3=n} \underline{\epsilon_{ijk}\epsilon_{pqr}\,\Psi^{(m_1)}_{i,p}\Psi^{(m_2)}_{j,q}\left(\frac{\partial^2}{\partial\eta^2}+\frac{1}{2}\frac{\partial}{\partial\eta}-\frac{1}{2}\right)\Psi^{(m_3)}_{k,r}},$$

vanished in 1D

vanished in 2D

Transverse: $$\epsilon_{ijk}\left(\frac{\partial^2}{\partial\eta^2}+\frac{1}{2}\frac{\partial}{\partial\eta}\right)\Psi^{(n)}_{j,k} = -\sum_{m_1+m_2=n} \underline{\epsilon_{ijk}\,\Psi^{(m_1)}_{p,j}\left(\frac{\partial^2}{\partial\eta^2}+\frac{1}{2}\frac{\partial}{\partial\eta}\right)\Psi^{(m_2)}_{p,k}}.$$

vanished in 1D

Zel'dovich solution: 1st-order LPT

$$\boldsymbol{\Psi}^{(1)} = \boldsymbol{\Psi}^{(1L)} + \boldsymbol{\Psi}^{(1T)} \ \ ;$$

$\eta \equiv \ln D_1(t)$

$$\left(\frac{\partial^2}{\partial\eta^2} + \frac{1}{2}\frac{\partial}{\partial\eta} - \frac{3}{2}\right)\Psi^{(1L)}_{k,k} = 0$$

$$\left(\frac{\partial^2}{\partial\eta^2} + \frac{1}{2}\frac{\partial}{\partial\eta}\right)\epsilon_{ijk}\Psi^{(1T)}_{j,k} = 0$$

Zel'dovich approximation : $\boldsymbol{\Psi}^{(1T)} = 0$ and take growing-mode only

$$\boldsymbol{\Psi}^{(1)} = \boldsymbol{\Psi}^{(1L)} = -\,D_1(a)\,\nabla_q\varphi(\boldsymbol{q}), \qquad \nabla_q^2\varphi(\boldsymbol{q}) = \delta_0(\boldsymbol{q})$$

: initial density field

$$\because \quad 1+\delta_{\rm m}(\boldsymbol{x}) = \left|\frac{\partial\boldsymbol{x}}{\partial\boldsymbol{q}}\right|^{-1} \equiv \frac{1}{J} \simeq \ 1 - \nabla_q\cdot\boldsymbol{\psi}$$

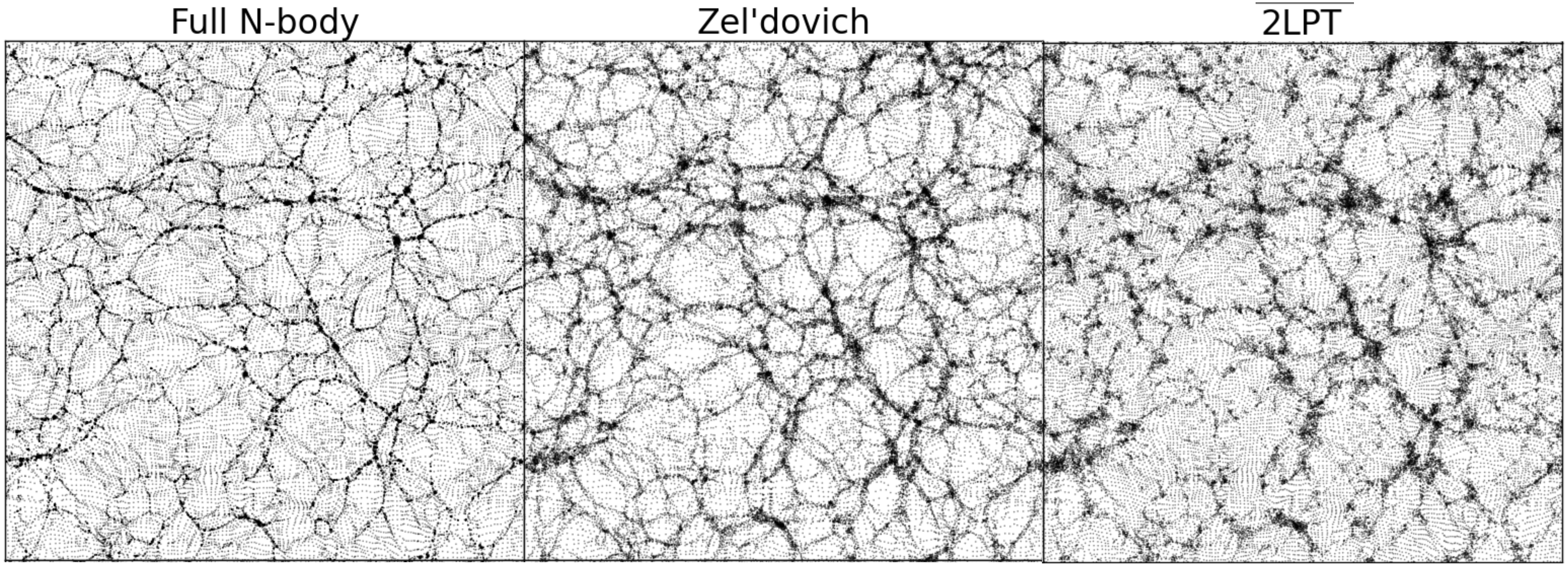

N_particle = 256^3

L=200Mpc/h

ΛCDM

power spectrum

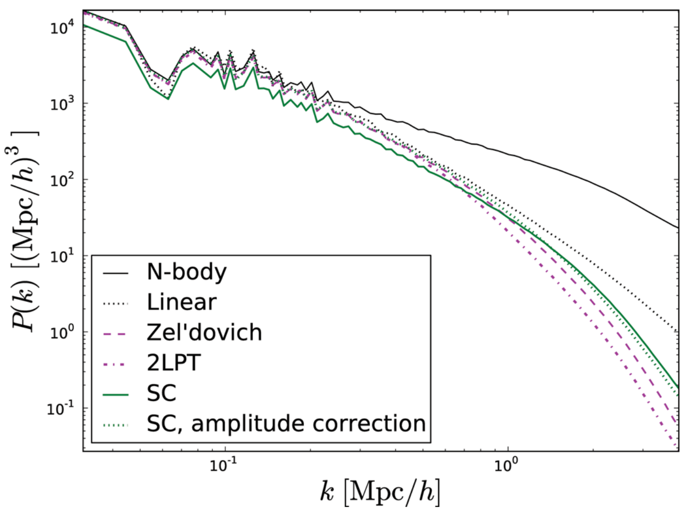

cross correlation coeff.

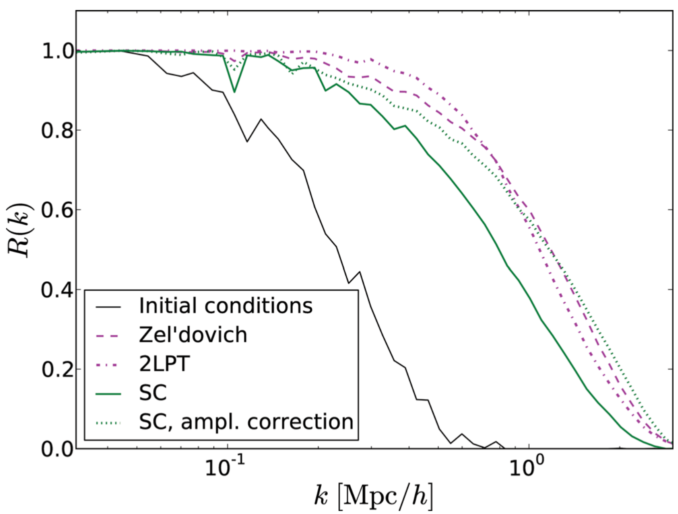

Neyrink ('13)

Particle trajectories in ZA

ZA

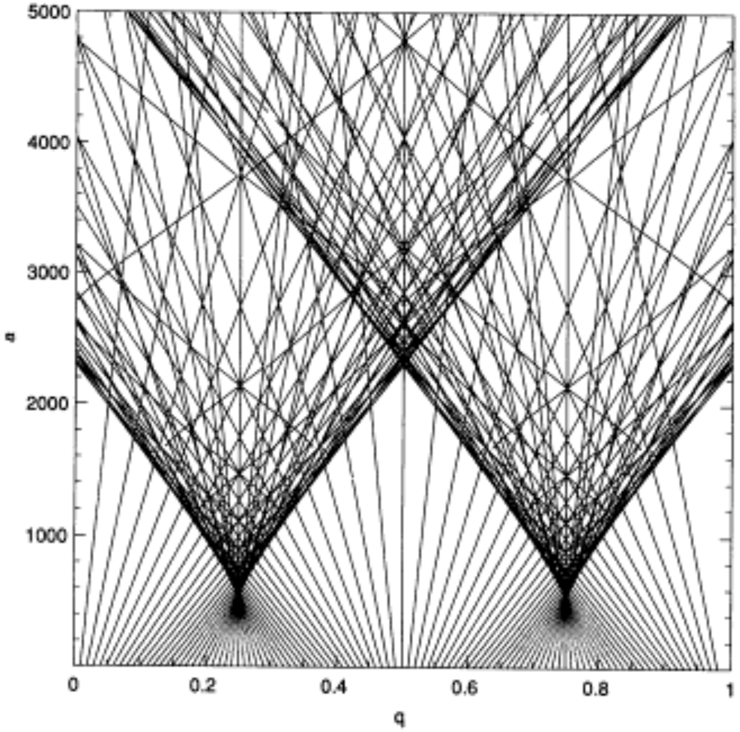

2LPT

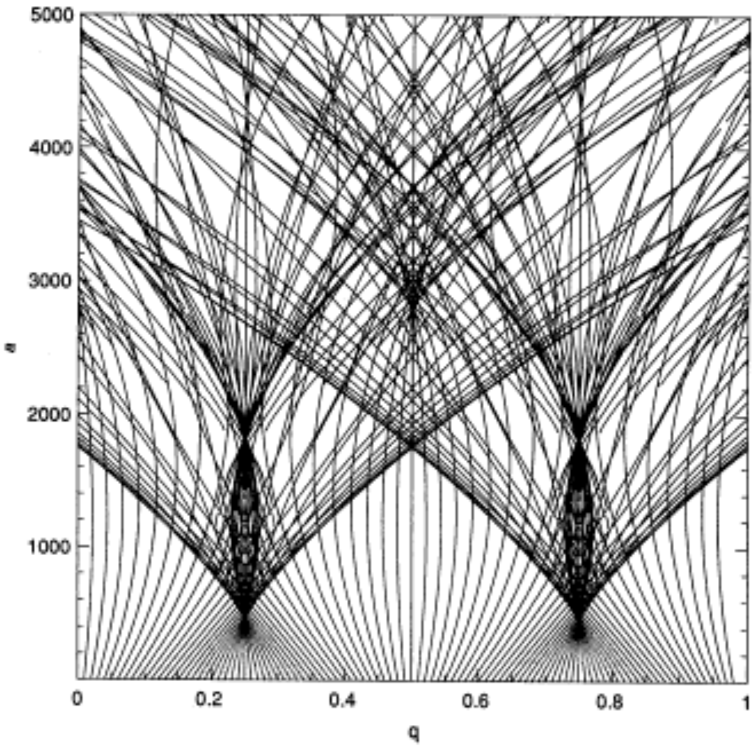

Figure 3. A family of trajectories corresponding to the model presented in Fig. 1 is shown for the first-order (upper panel) and second-order (lower panel) approximations. The trajectories end in the Eulerian space–time section ($y=0.5$, t) centred at a cluster. These plots illustrate that the three-stream system that develops after the first shell-crossing performs a self-oscillation due to the action of self-gravity.

Buchert & Ehlers ('93)

Higher-order solutions

For specific initial condition at t_0,

$$\boldsymbol{\Psi}^{(1)}(\boldsymbol{q},\, t_0) = D_1(t_0) \begin{pmatrix} \epsilon_{\mathrm{x}} \sin\, q_x \\ \epsilon_{\mathrm{y}} \sin\, q_y \\ \epsilon_{\mathrm{z}} \sin\, q_z \end{pmatrix}$$

$$\boldsymbol{\Psi}^{(n)} = 0, \quad \text{for} \;\; n \geq 2$$

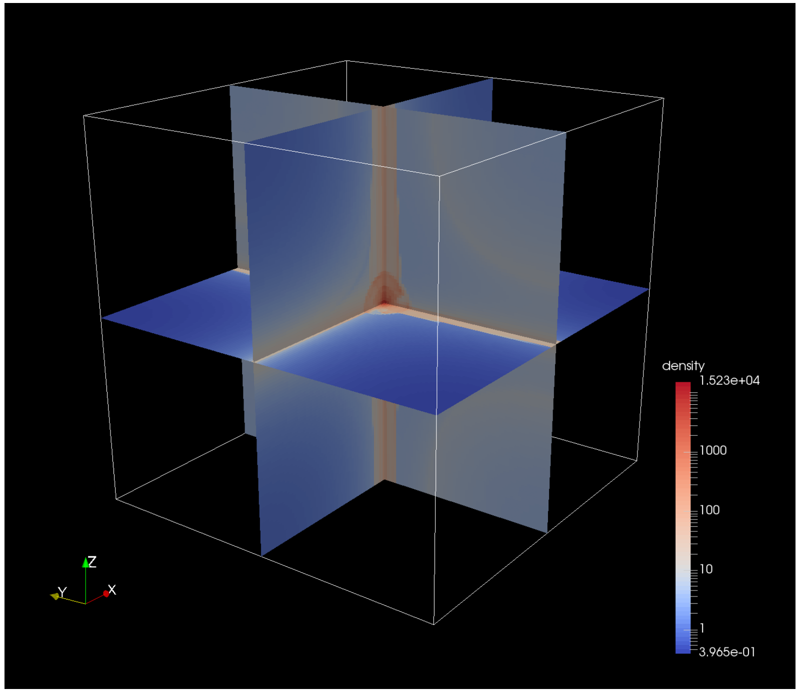

We derive LPT solutions at

2nd, 3rd, and 4th order

(W/ S. Saga)

(see Moutarde et al. '91 for similar work, but up to 3rd order)

2nd-order LPT

Longitudinal part only : $\nabla_q \times \mathbf{\Psi}^{(2)} = 0$

$$\mathbf{\Psi}^{(2)}(\boldsymbol{q},\, t) = D_2(t) \begin{pmatrix} \epsilon_{\rm x}\ \sin q_x(\epsilon_{\rm y} \cos q_y + \epsilon_{\rm z} \cos q_z) \\ \epsilon_{\rm y}\ \sin q_y(\epsilon_{\rm z} \cos q_z + \epsilon_{\rm x} \cos q_x) \\ \epsilon_{\rm z}\ \sin q_z(\epsilon_{\rm x} \cos q_x + \epsilon_{\rm y} \cos q_y) \end{pmatrix}$$

(Time-dependent) growth function:

$$D_2(t) = -\frac{3}{14}\, e^{2\eta} + \frac{3}{10}\, e^{\eta+\eta_0} - \frac{3}{35}\, e^{-(3/2)\eta+(7/2)\eta_0},$$

$$\eta \equiv \ln D_1(t)$$

3rd-order LPT

$$\boldsymbol{\Psi}^{(3)} = \boldsymbol{\Psi}^{(3L)} + \boldsymbol{\Psi}^{(3T)} \quad ;$$

Longitudinal

$$\boldsymbol{\Psi}^{(3L)}(\boldsymbol{q},\, t) = D_3(t)\,\boldsymbol{d}^{(3)}(\boldsymbol{q}) + E_3(t)\,\boldsymbol{e}^{(3)}(\boldsymbol{q});$$

$$\boldsymbol{d}^{(3)} = \frac{1}{5}\begin{pmatrix} \epsilon_{\rm x}\sin q_x\,(\epsilon_{\rm y}^2\cos^2 q_y + \epsilon_{\rm z}^2\cos^2 q_z) \\ \epsilon_{\rm y}\sin q_y\,(\epsilon_{\rm z}^2\cos^2 q_z + \epsilon_{\rm x}^2\cos^2 q_x) \\ \epsilon_{\rm z}\sin q_z\,(\epsilon_{\rm x}^2\cos^2 q_x + \epsilon_{\rm y}^2\cos^2 q_y) \end{pmatrix} + \frac{1}{5}\begin{pmatrix} \epsilon_{\rm x}^2\sin 2q_x\,(\epsilon_{\rm y}\cos q_y + \epsilon_{\rm z}\cos q_z) \\ \epsilon_{\rm y}^2\sin 2q_y\,(\epsilon_{\rm z}\cos q_z + \epsilon_{\rm x}\cos q_x) \\ \epsilon_{\rm z}^2\sin 2q_z\,(\epsilon_{\rm x}\cos q_x + \epsilon_{\rm y}\cos q_y) \end{pmatrix}$$

$$+\frac{2}{5}\begin{pmatrix} (\epsilon_{\rm y}^2 + \epsilon_{\rm z}^2)\,\epsilon_{\rm x}\sin q_x \\ (\epsilon_{\rm z}^2 + \epsilon_{\rm x}^2)\,\epsilon_{\rm y}\sin q_y \\ (\epsilon_{\rm x}^2 + \epsilon_{\rm y}^2)\,\epsilon_{\rm z}\sin q_z \end{pmatrix} + \boldsymbol{e}^{(3)}$$

$$\boldsymbol{e}^{(3)} = \begin{pmatrix} 2\epsilon_{\rm x}\epsilon_{\rm y}\epsilon_{\rm z}\ \sin q_x\cos q_y\cos q_z \\ 2\epsilon_{\rm x}\epsilon_{\rm y}\epsilon_{\rm z}\ \cos q_x\sin q_y\cos q_z \\ 2\epsilon_{\rm x}\epsilon_{\rm y}\epsilon_{\rm z}\ \cos q_x\cos q_y\sin q_z \end{pmatrix}$$

Transverse

$$\boldsymbol{\Psi}^{(3T)}(\boldsymbol{q},\, t) = F_3(t)\,\boldsymbol{f}^{(3)}(\boldsymbol{q});$$

$$\boldsymbol{f}^{(3)} = \frac{1}{10}\begin{pmatrix} \epsilon_{\rm x}^2\sin 2q_x\,(\epsilon_{\rm y}\cos q_y + \epsilon_{\rm z}\cos q_z) \\ \epsilon_{\rm y}^2\sin 2q_y\,(\epsilon_{\rm z}\cos q_z + \epsilon_{\rm x}\cos q_x) \\ \epsilon_{\rm z}^2\sin 2q_z\,(\epsilon_{\rm x}\cos q_x + \epsilon_{\rm y}\cos q_y) \end{pmatrix} - \frac{1}{5}\begin{pmatrix} \epsilon_{\rm x}\sin q_x\,(\epsilon_{\rm y}^2\cos 2q_y + \epsilon_{\rm z}^2\cos 2q_z) \\ \epsilon_{\rm y}\sin q_y\,(\epsilon_{\rm z}^2\cos 2q_z + \epsilon_{\rm x}^2\cos 2q_x) \\ \epsilon_{\rm z}\sin q_z\,(\epsilon_{\rm x}^2\cos 2q_x + \epsilon_{\rm y}^2\cos 2q_y) \end{pmatrix}$$

3rd-order LPT

Growth functions

$$D_3(\eta) = \frac{5}{42}\,e^{3\eta} - \frac{9}{70}\,e^{2\eta+\eta_0} - \frac{3}{35}\,e^{-\eta/2+(7/2)\eta_0} + \frac{2}{21}\,e^{-(3/2)\eta+(9/2)\eta_0},$$

$$E_3(\eta) = -\frac{1}{18}\,e^{3\eta} + \frac{1}{10}\,e^{\eta+2\eta_0} - \frac{2}{45}\,e^{-(3/2)\eta+(9/2)\eta_0},$$

$$F_3(t) = \frac{1}{14}\,e^{3\eta} - \frac{1}{2}\,e^{3\eta_0} + \frac{3}{7}\,e^{-\eta/2+(7/2)\eta_0}$$

$$\eta \equiv \ln D_1(t)$$

4th-order LPT (x-component)

Longitudinal

$$\boldsymbol{\Psi}^{(4L)}(\boldsymbol{q},\, t) = D_4(t)\,\boldsymbol{d}^{(4)}(\boldsymbol{q}) + E_4(t)\,\boldsymbol{e}^{(4)}(\boldsymbol{q}) \ + F_4(t)\,\boldsymbol{f}^{(4)}(\boldsymbol{q}) + G_4(t)\,\boldsymbol{g}^{(4)}(\boldsymbol{g}) + H_4(t)\,\boldsymbol{h}^{(4)}(\boldsymbol{g});$$

$$\begin{aligned}
d_x^{(4)} &= \frac{1}{2}\epsilon_{\rm x}\sin q_x\big(2\epsilon_{\rm x}\cos q_x\big(2\epsilon_{\rm y}\cos q_y\epsilon_{\rm z}\cos q_z \ +\epsilon_{\rm y}^2+\epsilon_{\rm z}^2\big)+\epsilon_{\rm y}\epsilon_{\rm z}\big(\epsilon_{\rm y}(\cos(2q_y)+3)\cos q_z \\
&\quad +\epsilon_{\rm z}\cos q_y(\cos(2q_z)+3)\big)\big) \\
e_x^{(4)} &= \frac{1}{100}\epsilon_{\rm x}\sin q_x\big(20\epsilon_{\rm x}\cos q_x\big(10\epsilon_{\rm y}\cos q_y\epsilon_{\rm z}\cos q_z \ +\epsilon_{\rm y}^2+\epsilon_{\rm y}^2\cos(2q_y)+\epsilon_{\rm z}^2+\epsilon_{\rm z}^2\cos(2q_z)\big) \\
&\qquad +\epsilon_{\rm z}\cos(q_z)\big(29\epsilon_{\rm x}^2+3\epsilon_{\rm x}^2\cos(2q_x)+150\epsilon_{\rm y}^2+50\epsilon_{\rm y}^2\cos(2q_y)+27\epsilon_{\rm z}^2+\epsilon_{\rm z}^2\cos(2q_z)\big) \\
&\qquad +\epsilon_{\rm y}\cos q_y\big(29\epsilon_{\rm x}^2+3\epsilon_{\rm x}^2\cos(2q_x)+27\epsilon_{\rm y}^2 \ +\epsilon_{\rm y}^2\cos(2q_y)+150\epsilon_{\rm z}^2+50\epsilon_{\rm z}^2\cos(2q_z)\big)\big) \\
f_x^{(4)} &= \frac{1}{6}\epsilon_{\rm x}\sin q_x\epsilon_{\rm y}\epsilon_{\rm z}\big(2\cos q_y\big(4\epsilon_{\rm x}\cos q_x\cos q_z+\epsilon_{\rm z}(\cos(2q_z)+3)\big)+2\epsilon_{\rm y}\cos^2 q_y\cos q_z \\
&\qquad +\epsilon_{\rm y}(\cos(2q_y)+5)\cos q_z\big) \\
g_x^{(4)} &= -\frac{1}{50}\epsilon_{\rm x}\sin q_x\big(-5\epsilon_{\rm x}\cos q_x\big(\epsilon_{\rm y}^2\cos(2q_y)+\epsilon_{\rm z}^2\cos(2q_z)+\epsilon_{\rm y}^2+\epsilon_{\rm z}^2\big)+\epsilon_{\rm y}\cos q_y \\
&\quad \times\ \big(3\epsilon_{\rm x}^2\cos(2q_x)+\epsilon_{\rm y}^2\cos(2q_y)+4\epsilon_{\rm x}^2+2\epsilon_{\rm y}^2\big)+\epsilon_{\rm z}\cos q_z\big(3\epsilon_{\rm x}^2\cos(2q_x)+\epsilon_{\rm z}^2\cos(2q_z) \\
&\quad +4\epsilon_{\rm x}^2+2\epsilon_{\rm z}^2\big)\big) \\
h_x^{(4)} &= \frac{1}{6}\epsilon_{\rm x}\epsilon_{\rm y}\epsilon_{\rm z}\sin q_x\big(2\cos q_y\big(4\epsilon_{\rm x}\cos q_x\cos q_z+\epsilon_{\rm z}\big(\cos(2q_z)+3\big)\big)+2\epsilon_{\rm y}\cos^2 q_y\cos q_z \\
&\quad +\epsilon_{\rm y}\big(\cos(2q_y)+5\big)\cos q_z\big)
\end{aligned}$$

4th-order LPT (x-component)

Transverse

$$\boldsymbol{\Psi}^{(4T)}(\boldsymbol{q},\, t) = I_4(t)\, \boldsymbol{i}^{(4)}(\boldsymbol{q}) + J_4(t)\, \boldsymbol{j}^{(4)}(\boldsymbol{q}) + K_4(t)\, \boldsymbol{k}^{(4)}(\boldsymbol{q});$$

$$\begin{aligned}
i_x^{(4)} &= \frac{1}{150}\epsilon_{\mathrm{x}} \sin q_x \big(\epsilon_{\mathrm{y}} \cos q_y \big(100\epsilon_{\mathrm{x}}\epsilon_{\mathrm{z}} \cos q_x \cos q_z + 3\epsilon_{\mathrm{x}}^2 \cos(2q_x) - 9\epsilon_{\mathrm{y}}^2 \cos(2q_y) - 50\epsilon_{\mathrm{z}}^2 \cos(2q_z) \\
&\quad + 9\epsilon_{\mathrm{x}}^2 - 3\epsilon_{\mathrm{y}}^2\big) + \epsilon_{\mathrm{z}} \cos q_z \big(3\epsilon_{\mathrm{x}}^2 \cos(2q_x) - 50\epsilon_{\mathrm{y}}^2 \cos(2q_y) - 9\epsilon_{\mathrm{z}}^2 \cos(2q_z) + 9\epsilon_{\mathrm{x}}^2 - 3\epsilon_{\mathrm{z}}^2\big)\big)
\end{aligned}$$

$$j_x^{(4)} = \frac{1}{3}\epsilon_{\mathrm{x}}\epsilon_{\mathrm{y}}\epsilon_{\mathrm{z}} \sin q_x \big(2\epsilon_{\mathrm{x}} \cos q_x \cos q_y \cos q_z - \epsilon_{\mathrm{y}} \cos(2q_y) \cos q_z - \epsilon_{\mathrm{z}} \cos q_y \cos(2q_z)\big)$$

$$\begin{aligned}
k_x^{(4)} &= \frac{1}{100}\epsilon_{\mathrm{x}} \sin q_x \big(\epsilon_{\mathrm{z}} \cos q_z \big(\epsilon_{\mathrm{x}}^2 \cos(2q_x) - 3\epsilon_{\mathrm{z}}^2 \cos(2q_z) + 3\epsilon_{\mathrm{x}}^2 - \epsilon_{\mathrm{z}}^2\big) - \epsilon_{\mathrm{y}} \cos q_y \\
&\quad \times \big(-\epsilon_{\mathrm{x}}^2 \cos(2q_x) + 3\epsilon_{\mathrm{y}}^2 \cos(2q_y) - 3\epsilon_{\mathrm{x}}^2 + \epsilon_{\mathrm{y}}^2\big)\big)
\end{aligned}$$

4th-order LPT (time dependence)

$$D_4(\eta) = -\frac{51}{4312}\,e^{4\eta} + \frac{1}{28}\,e^{3\eta+\eta_0} - \frac{27}{1400}\,e^{2\eta+2\eta_0} - \frac{3}{40}e^{\eta+3\eta_0} + \frac{9}{98}e^{\eta/2+(7/2)\eta_0} - \frac{9}{350}e^{-\eta/2+(9/2)\eta_0} + \frac{2}{385}e^{-(3/2)\eta+(11/2)\eta_0} - \frac{9}{9800}e^{-3\eta+7\eta_0}$$

$$E_4(\eta) = -\frac{5}{66}\,e^{4\eta} + \frac{1}{14}\,e^{3\eta+\eta_0} + \frac{2}{21}\,e^{-\eta/2+(9/2)\eta_0} - \frac{1}{11}e^{-(3/2)\eta+(11/2)\eta_0}$$

$$F_4(\eta) = \frac{7}{198}e^{4\eta} - \frac{3}{70}e^{2\eta+2\eta_0} - \frac{2}{45}e^{-\eta/2+(9/2)\eta_0} + \frac{4}{77}e^{-(3/2)\eta+(11/2)\eta_0}$$

$$G_4(\eta) = -\frac{1}{22}\,e^{4\eta} + \frac{1}{10}\,e^{\eta+3\eta_0} - \frac{3}{55}\,e^{-(3/2)\eta+(11/2)\eta_0}$$

$$H_4(\eta) = \frac{13}{308}e^{4\eta} - \frac{1}{20}e^{3\eta+\eta_0} + \frac{1}{10}e^{\eta+3\eta_0} - \frac{9}{70}e^{\eta/2+(7/2)\eta_0} + \frac{2}{55}e^{-(3/2)\eta+(11/2)\eta_0}$$

$$I_4(\eta) = -\frac{5}{84}\,e^{4\eta} + \frac{3}{70}\,e^{3\eta+\eta_0} - \frac{9}{35}\,e^{(1/2)\eta+(7/2)\eta_0} + \frac{3}{4}e^{4\eta_0} - \frac{10}{21}e^{-\eta/2+(9/2)\eta_0}$$

$$J_4(\eta) = \frac{1}{36}e^{4\eta} - \frac{1}{4}e^{4\eta_0} + \frac{2}{9}e^{-\eta/2+(9/2)\eta_0}$$

$$K_4(\eta) = -\frac{1}{28}\,e^{4\eta} - \frac{1}{2}\,e^{\eta+3\eta_0} + \frac{9}{7}\,e^{(1/2)\eta+(7/2)\eta_0} - \frac{3}{4}e^{4\eta_0}$$

$$\eta \equiv \ln D_1(t)$$

Comparison with Vlasov simulation

Vlasov simulation:
S. Colombi

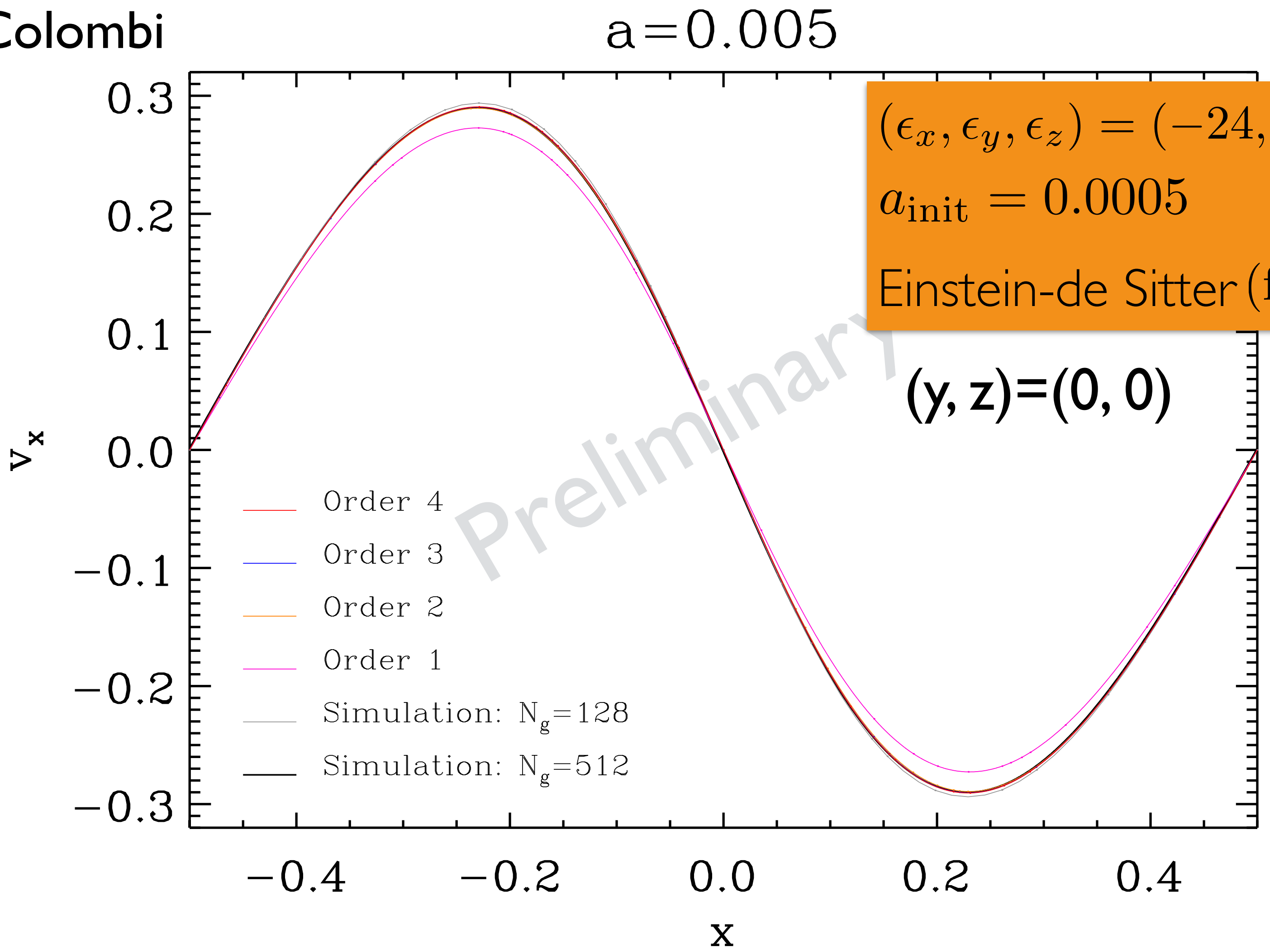

$(\epsilon_x, \epsilon_y, \epsilon_z) = (-24, -18, -12)$

$a_{\rm init} = 0.0005$

Einstein-de Sitter $(\text{flat}, \ \Omega_{\rm m} = 1)$

Comparison with Vlasov simulation

Vlasov simulation:
S. Colombi

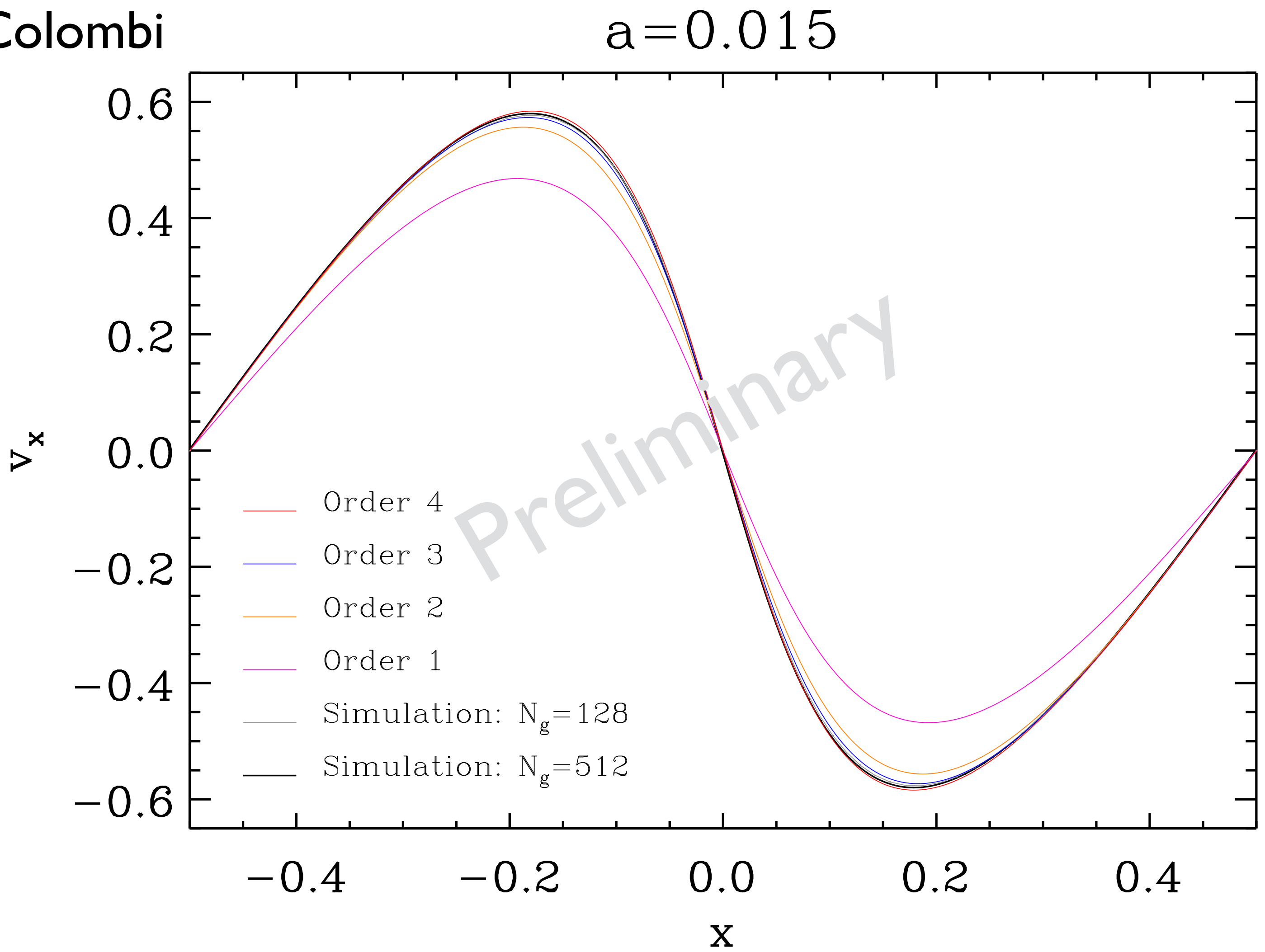

Comparison with Vlasov simulation

Vlasov simulation:
S. Colombi

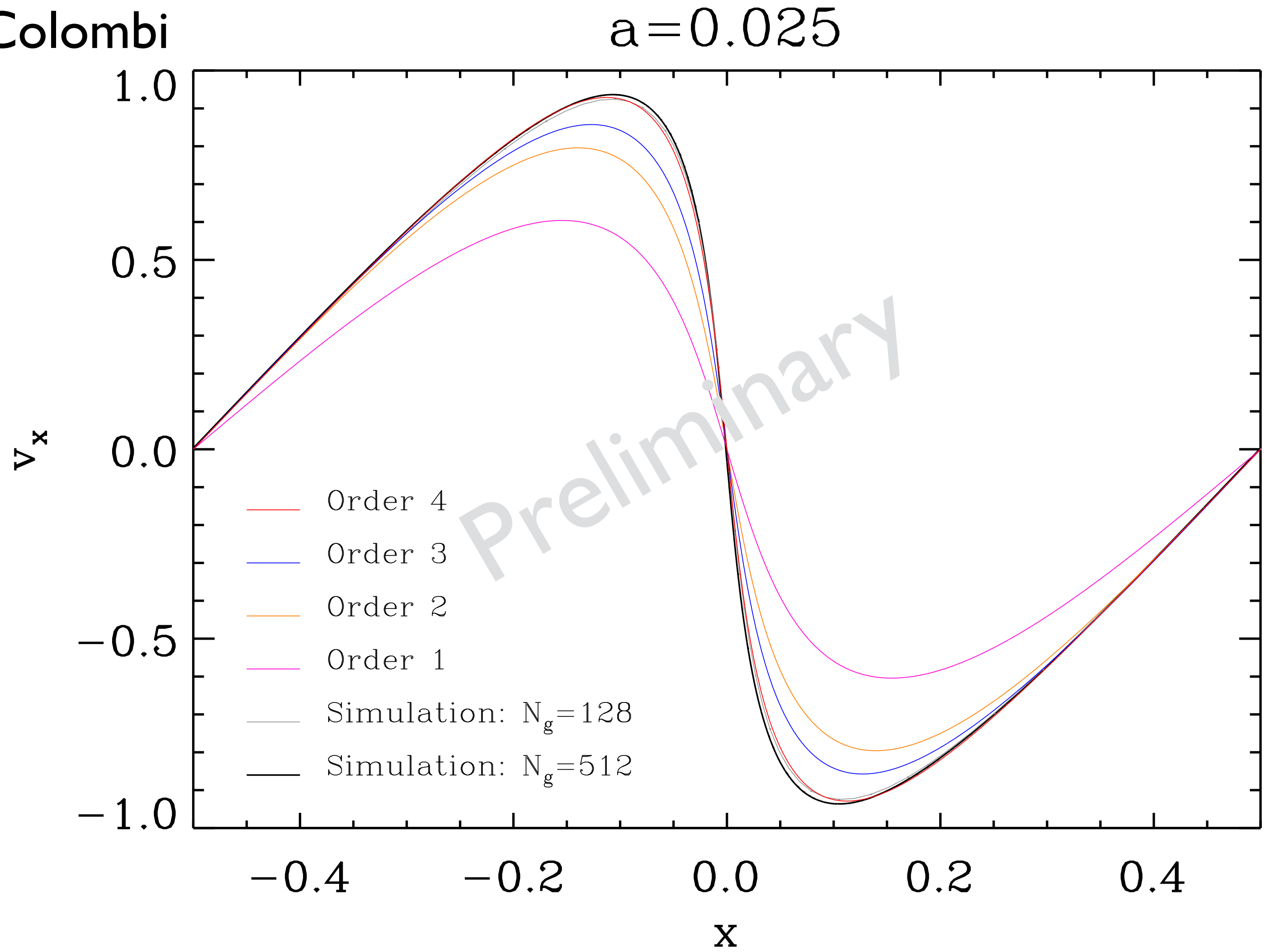

Comparison with Vlasov simulation

Vlasov simulation:
S. Colombi

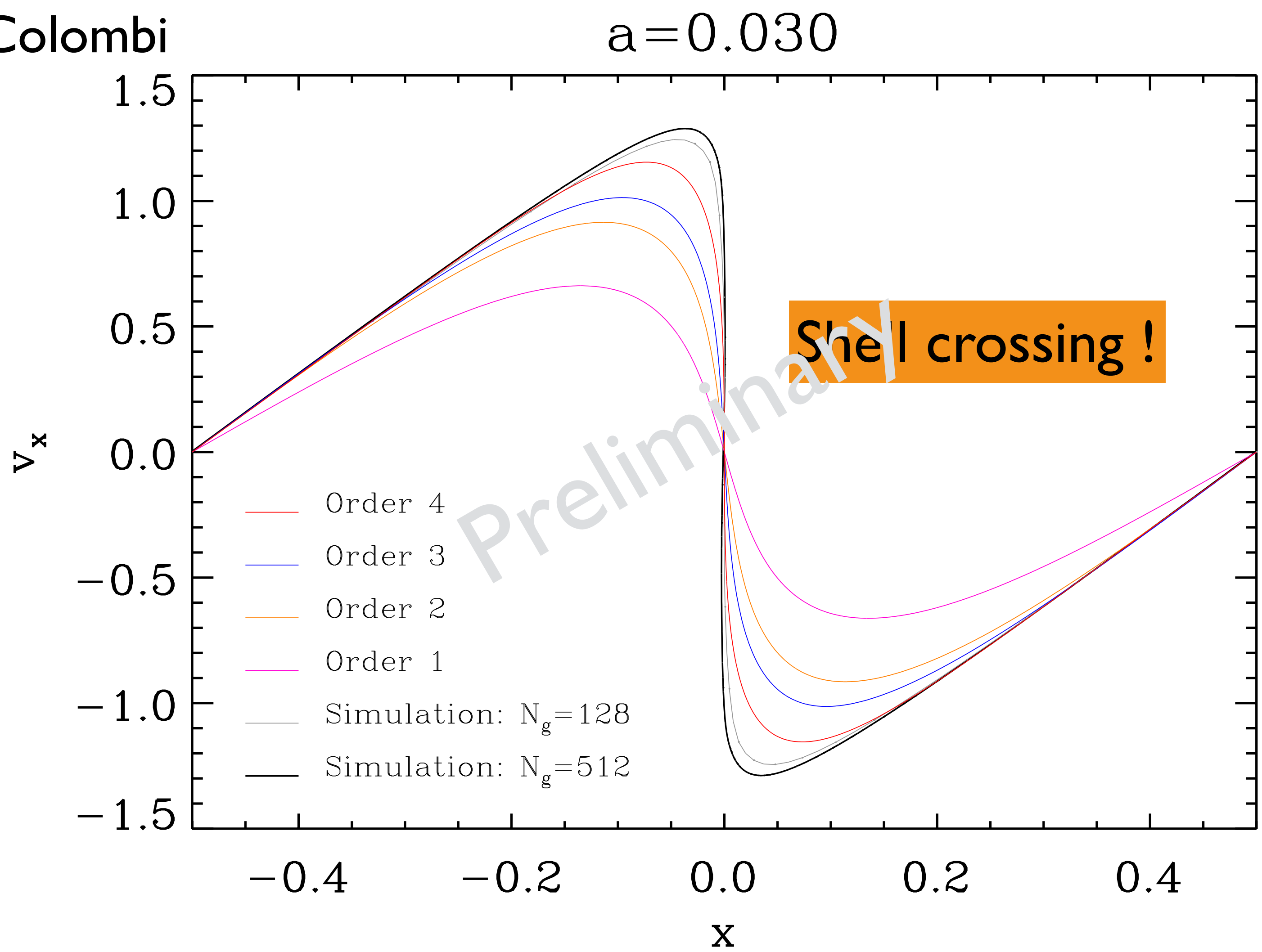

Comparison with Vlasov simulation

Vlasov simulation:
S. Colombi

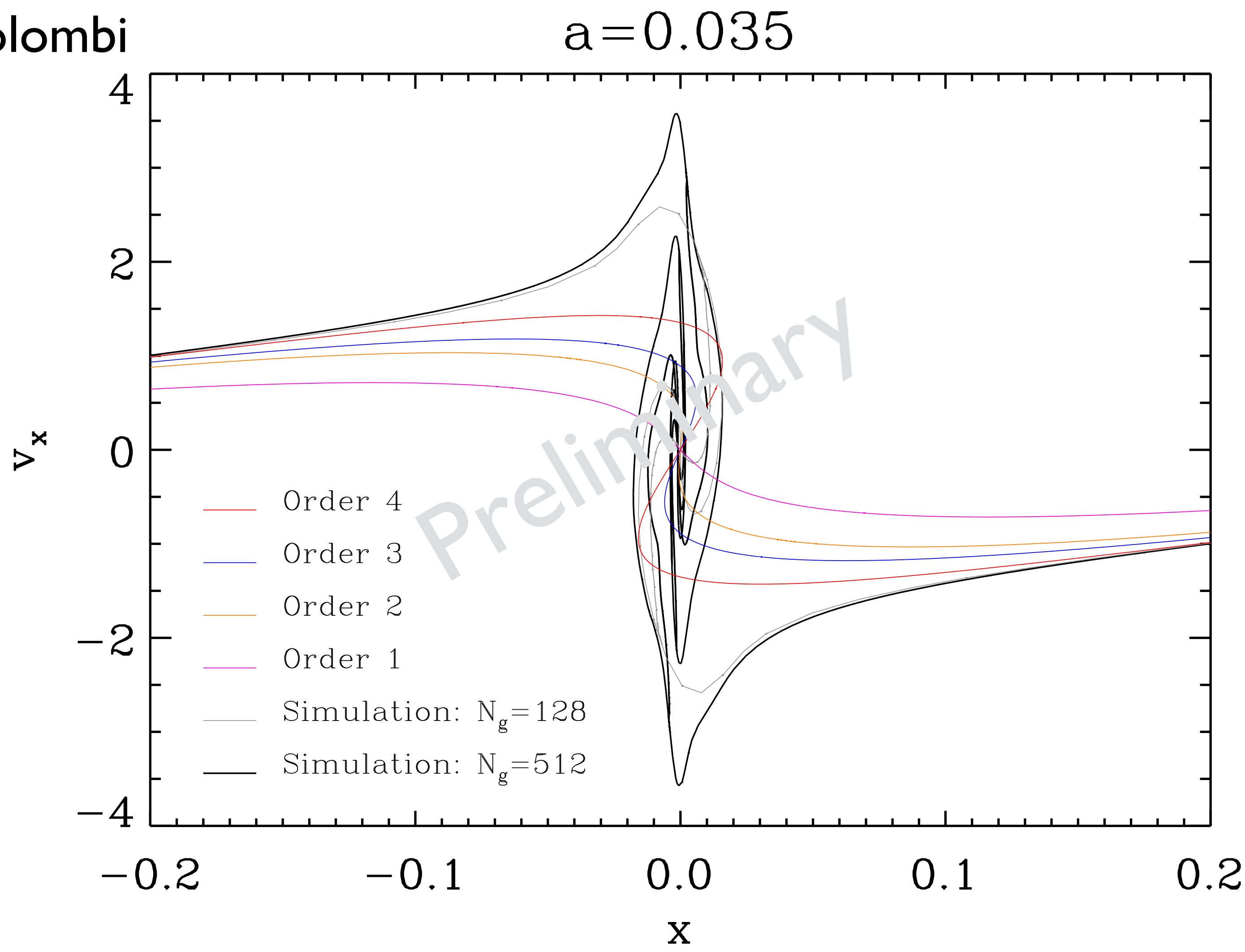

Vlasov simulation

Vlasov simulation:
S. Colombi

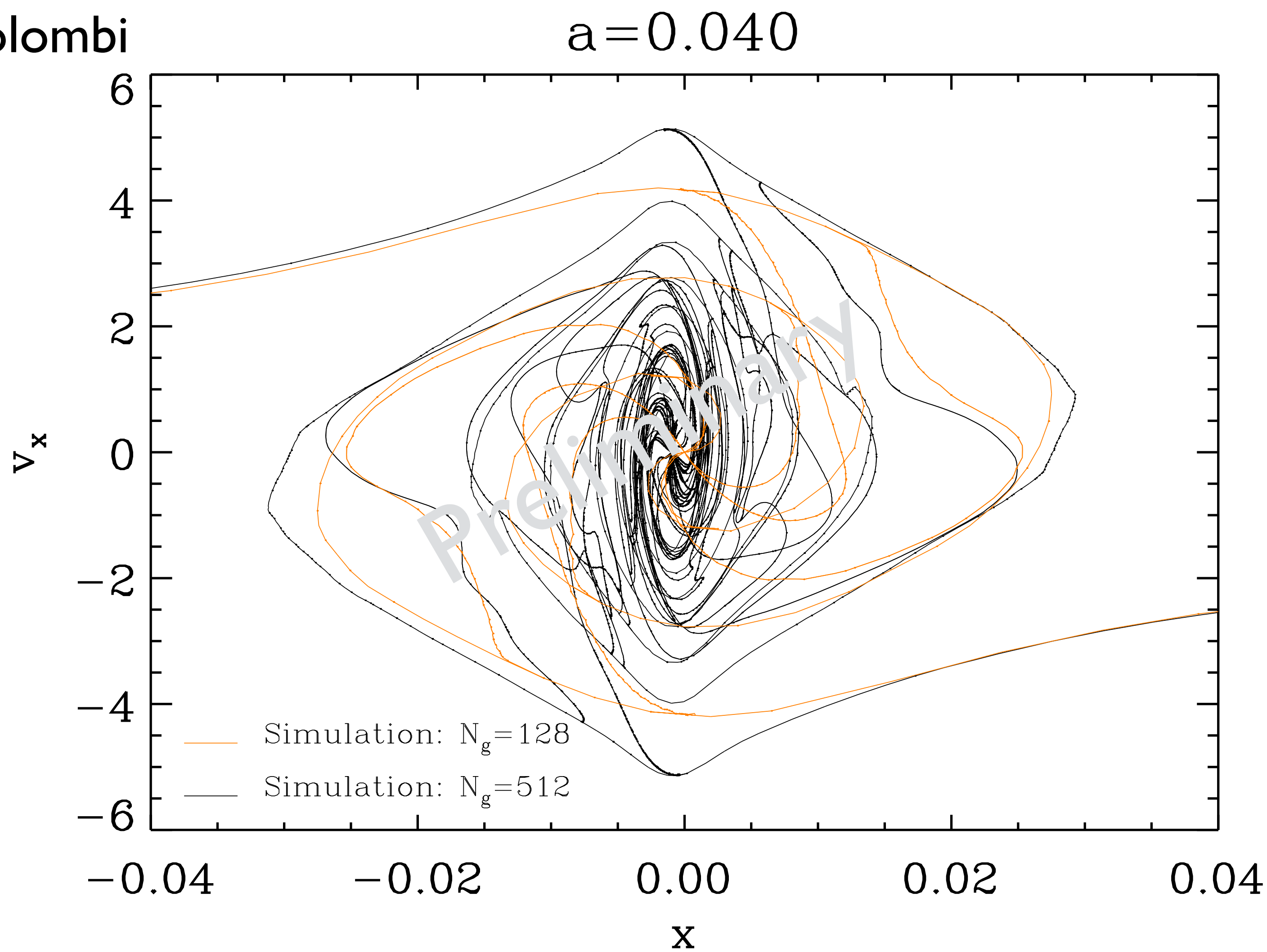

Summary

Perturbation theory (PT) of large-scale structure has been developed as a precision tool, but it needs to be renovated

✓ UV issue in single-stream PT: Do not go to 3-loop !

✓ Response function: Characterizing nature of mode coupling

✓ Post-collapse PT with adaptive smoothing in 1D:
Novel scheme beyond shell crossing

✓ Roadmap to 3D: pre-collapse evolution from LPT and
Vlasov simulation

Stay tuned, and
do not stick to Effective-field-theory approach !